

The Local Fractional Bootstrap*

Mikkel Bennedsen[†] Ulrich Hounyo[‡] Asger Lunde[§] Mikko S. Pakkanen[¶]

November 8, 2021

Abstract

We introduce a bootstrap procedure for high-frequency statistics of Brownian semistationary processes. More specifically, we focus on a hypothesis test on the roughness of sample paths of Brownian semistationary processes, which uses an estimator based on a ratio of realized power variations. Our new resampling method, the local fractional bootstrap, relies on simulating an auxiliary fractional Brownian motion that mimics the fine properties of high frequency differences of the Brownian semistationary process under the null hypothesis. We prove the first order validity of the bootstrap method and in simulations we observe that the bootstrap-based hypothesis test provides considerable finite-sample improvements over an existing test that is based on a central limit theorem. This is important when studying the roughness properties of time series data; we illustrate this by applying the bootstrap method to two empirical data sets: we assess the roughness of a time series of high-frequency asset prices and we test the validity of Kolmogorov’s scaling law in atmospheric turbulence data.

Keywords: Brownian semistationary process; roughness; fractal index; Hölder regularity; fractional Brownian motion; bootstrap; stochastic volatility; turbulence.

JEL Classification: C12, C22, C63, G12

MSC 2010 Classification: 60G10, 60G15, 60G17, 60G22, 62M07, 62M09, 65C05

1 Introduction

In the study of pathwise properties of continuous stochastic processes, *roughness* is a central attribute. Theoretically, roughness relates to the degree of Hölder regularity enjoyed by the sample

*We would like to thank Solveig Sørensen for competent and precise proof reading of the manuscript. Our research has been supported by CREATES (DNRF78), funded by the Danish National Research Foundation, by Aarhus University Research Foundation (project “Stochastic and Econometric Analysis of Commodity Markets”), and by the Academy of Finland (project 258042).

[†]Department of Economics and Business Economics and CREATES, Aarhus University, Fuglesangs Allé 4, 8210 Aarhus V, Denmark. E-mail: mbennedsen@econ.au.dk

[‡]Department of Economics and Business Economics and CREATES, Aarhus University, Fuglesangs Allé 4, 8210 Aarhus V, Denmark. E-mail: uhounyo@econ.au.dk

[§]Department of Economics and Business Economics and CREATES, Aarhus University, Fuglesangs Allé 4, 8210 Aarhus V, Denmark. E-mail: alunde@econ.au.dk

[¶]Department of Mathematics, Imperial College London, South Kensington Campus, London SW7 2AZ, UK and CREATES, Aarhus University, Denmark. E-mail: m.pakkanen@imperial.ac.uk

paths of the stochastic process in question. The fractional Brownian motion (fBm), introduced by Kolmogorov (1940) and popularized later by Mandelbrot and Van Ness (1968), is perhaps the most well-known example of a process that can exhibit various degrees of roughness. The fBm with Hurst index $H \in (0, 1)$ is a Gaussian process that coincides with the standard Brownian motion when $H = 1/2$. If $H < 1/2$ (respectively $H > 1/2$), then the sample paths of the fBm are rougher (respectively smoother) than those of the standard Brownian motion in terms of Hölder regularity. In this work, we are concerned with conducting inference on the *fractal index*, α , of a stochastic process, when α is estimated using the so-called *change-of-frequency* (COF) estimator, introduced by Lang and Roueff (2001) for Gaussian processes and extended by Barndorff-Nielsen et al. (2013) and Corcuera et al. (2013) to a non-Gaussian setting. In the case of the fBm it holds that $\alpha = H - 1/2$, whilst in general $\alpha < 0$ indicates roughness and $\alpha > 0$ smoothness relative to the standard Brownian motion, as with fBm. When $\alpha = 0$, the stochastic process under consideration has the same roughness as the standard Brownian motion.

Several interesting empirical time series exhibit signs of roughness, i.e. $\alpha < 0$. Some noteworthy examples include:

- time-wise measurements of velocity in turbulent flows (Corcuera et al., 2013), where roughness in inertial time scales is predicted by Kolmogorov’s scaling law (Kolmogorov, 1941) and Taylor’s *frozen field hypothesis* (Taylor, 1938),
- time series of electricity spot prices (Barndorff-Nielsen et al., 2013; Bennedsen, 2017),
- measures of the realized volatility of asset prices (Gatheral et al., 2014; Bennedsen et al., 2016).

In these applications, estimation of, and inference on, the index α is important. There is a long history of methods of estimating α , concentrating mostly on Gaussian processes, of which a comprehensive survey is provided in Gneiting et al. (2012). In the time series data mentioned above, non-Gaussian features are pervasive, however, which is why we concentrate on a specific, yet flexible, non-Gaussian framework. *Brownian semistationary* (\mathcal{BSS}) processes (Barndorff-Nielsen and Schmiegel, 2007, 2009) form a class of stochastic processes that accommodate various departures from Gaussianity and different degrees of roughness. Barndorff-Nielsen et al. (2013) and Corcuera et al. (2013) and have studied the properties of the COF estimator of α in the context of \mathcal{BSS} processes. In particular, they have derived a central limit theorem (CLT), that makes it possible to conduct hypothesis tests on α .

In the present paper, our main focus will be on the COF estimator of a driftless \mathcal{BSS} process $(X_t)_{t \in \mathbb{R}}$, given by

$$X_t = \int_{-\infty}^t g(t-s)\sigma_s dW_s,$$

where $g : \mathbb{R}^+ \rightarrow \mathbb{R}$ is a kernel function, $(\sigma_t)_{t \in \mathbb{R}}$ a stochastic volatility process, and $(W_t)_{t \in \mathbb{R}}$ a standard Brownian motion. Important for our present purpose, we assume that the kernel function $g(x)$ behaves like a power function, $x \mapsto x^\alpha$, when x is near zero; a statement we will make precise below. When this assumption holds, and some additional (mild) technical conditions are met, the sample paths of X are Hölder continuous with index $\alpha + 1/2 - \varepsilon$ for any $\varepsilon > 0$ (Bennedsen et al., 2017, Proposition 2.1). Moreover, $\alpha = 0$ is a necessary condition for the process to be a semimartingale (Basse, 2008; Bennedsen, 2016). Intuitively, the \mathcal{BSS} process is a moving average process driven by volatility-modulated Brownian noise and is, thus, quite general and flexible. The \mathcal{BSS} framework is also closely related to processes such as the fBm and Gaussian Volterra processes of convolution type; see e.g. Bennedsen et al. (2017). Therefore we expect the methods proposed in this paper to apply to these processes as well, but research into the specifics is beyond the scope of the present paper and left for future work.

The contribution of this paper is to derive a bootstrap procedure that improves the finite sample properties of the test of the null hypothesis

$$H_0 : \alpha = \alpha_0,$$

for some $\alpha_0 \in (-\frac{1}{2}, \frac{1}{2})$, when the fractal index α is estimated using the COF estimator. Theoretically, the COF estimator has two regimes: in the first regime $\alpha \in (-\frac{1}{2}, \frac{1}{4})$, the estimator uses the entire sample to estimate α . In this case, we propose a novel bootstrap method, the *local fractional bootstrap*, which utilizes simulations of an auxiliary fractional Brownian motion with Hurst index $H = \alpha_0 + \frac{1}{2}$, thereby mimicking the fine properties of the sample paths of the underlying \mathcal{BSS} process under H_0 . We establish the first-order asymptotic validity of the local fractional bootstrap for the percentile- t methods, i.e. when the test-statistic is normalized by its (bootstrap) standard deviation.

As noted in Corcuera et al. (2013, Section 4), in the second regime $\alpha \in [\frac{1}{4}, \frac{1}{2})$, the asymptotic behavior of the COF estimator is potentially affected (depending on the form of g) by a non-negligible bias term, causing the CLT to break down. For this reason, the authors suggest using a modified COF estimator that implements asymptotically increasing gaps between increments from which the power variations are computed. These gaps make the increments used in the estimator asymptotically uncorrelated, which opens the door to a *wild bootstrap* approach (e.g. Wu, 1986; Liu, 1988; Gonçalves and Meddahi, 2009) in this regime. However, since the local fractional bootstrap method proposed in this paper works even when $\alpha \in [\frac{1}{4}, \frac{1}{2})$, we, for the sake of brevity, relegate the details on the wild bootstrap method, along with the simulation study of its finite sample properties, to a separate web appendix (Bennedsen et al., 2017).

In a Monte Carlo simulation study, we assess the finite sample properties of the local fractional bootstrap procedure in comparison with the inference method based on the CLT of Corcuera et al.

(2013). We find that for all $\alpha \in (-\frac{1}{2}, \frac{1}{2})$, the local fractional bootstrap offers improvements in terms of the size of the test of H_0 , especially when the sample size ranges from small to moderate. Indeed, since our method simulates the auxiliary bootstrap observations under H_0 , we minimize the probability of a type I error (Davidson and MacKinnon, 1999), i.e. of rejecting H_0 when it actually holds. This feature proves to be important when we in the empirical section apply the method to assess the roughness of the time series of logarithmic prices of the E-mini futures contract. In this case, no-arbitrage considerations suggest that $\alpha = 0$, and we find that the bootstrap procedure is crucial for achieving the correct size of the test of $H_0 : \alpha = 0$ when applied to intraday price series. We also apply the bootstrap method to a time series of measurements of atmospheric turbulence to test for the empirical validity of Kolmogorov’s scaling law (Kolmogorov, 1941). We find the data to be in good agreement with the scaling law, but again using the bootstrap is crucial for accurate inference when the sample size is small.

The rest of this paper is structured as follows. Section 2 sets the stage by presenting the mathematical definition of the \mathcal{BSS} process as well as the assumptions we work under. This section also briefly reviews existing results as they pertain to the present work. In Section 3 we detail our bootstrap method, the local fractional bootstrap, and give the details on its implementation. Section 4 contains a Monte Carlo study of the finite sample properties of the bootstrap method and Section 5 presents the empirical applications. Section 6 concludes. Simulation setup, proofs, as well as some additional technical derivations, are given in Appendices A, B, and C. The details on the wild bootstrap method, including proofs and a simulation experiment, are available in a web appendix (Bennedsen et al., 2017).

2 Setup, assumptions, and review of existing results

Now, we introduce some essential notation. Following the conventions of bootstrap literature, \mathbb{P}^* (\mathbb{E}^* and Var^*) denotes the probability measure (expected value and variance) induced by the bootstrap resampling, conditional on a realization of the original time series. In addition, for a sequence of bootstrap statistics Z_n^* , we write $Z_n^* = o_{p^*}(1)$ in probability, or $Z_n^* \xrightarrow{\mathbb{P}^*} 0$, as $n \rightarrow \infty$, in probability, if for any $\varepsilon > 0$, $\delta > 0$,

$$\lim_{n \rightarrow \infty} \mathbb{P} [\mathbb{P}^* (|Z_n^*| > \delta) > \varepsilon] = 0.$$

Similarly, we write $Z_n^* = O_{p^*}(1)$ as $n \rightarrow \infty$, in probability if for all $\varepsilon > 0$ there exists $M_\varepsilon < \infty$ such that

$$\lim_{n \rightarrow \infty} \mathbb{P} [\mathbb{P}^* (|Z_n^*| > M_\varepsilon) > \varepsilon] = 0.$$

Finally, we write $Z_n^* \xrightarrow{d^*} Z$ as $n \rightarrow \infty$, in probability, if conditional on the sample, Z_n^* converges weakly to Z under \mathbb{P}^* , for all samples contained in a set with \mathbb{P} -probability converging to one.

2.1 \mathcal{BSS} setup and assumptions

We follow [Barndorff-Nielsen et al. \(2013\)](#) and consider a filtered probability space $(\Omega, \mathcal{F}, (\mathcal{F}_t)_{t \in \mathbb{R}}, \mathbb{P})$, on which we define a Brownian semistationary (\mathcal{BSS}) process $X = (X_t)_{t \in \mathbb{R}}$, without a drift as

$$X_t = \int_{-\infty}^t g(t-s) \sigma_s dW_s, \quad t \in \mathbb{R}, \quad (1)$$

where $(W_t)_{t \in \mathbb{R}}$ is a two-sided standard Brownian motion, $g : \mathbb{R}^+ \rightarrow \mathbb{R}$ is a deterministic weight function satisfying $g \in L^2(\mathbb{R}^+)$, and $(\sigma_t)_{t \in \mathbb{R}}$ is an $(\mathcal{F}_t)_{t \in \mathbb{R}}$ -adapted càdlàg process. We assume that

$$\int_{-\infty}^t g^2(t-s) \sigma_s^2 ds < \infty \text{ a.s.}, \quad \text{for all } t \in \mathbb{R},$$

to ensure that X_t is a.s. finite for any $t \in \mathbb{R}$. We introduce a centered stationary Gaussian process $G = (G_t)_{t \in \mathbb{R}}$ that is associated to X , which we will call the *Gaussian core* of X , as

$$G_t = \int_{-\infty}^t g(t-s) dW_s, \quad t \in \mathbb{R}. \quad (2)$$

The correlation kernel r of G is given via

$$r(t) = \text{corr}(G_s, G_{s+t}) = \frac{\int_0^\infty g(u) g(u+t) du}{\|g\|_{L^2(\mathbb{R}^+)}^2}, \quad t \geq 0.$$

A crucial object in the asymptotic theory is the variogram R , given by

$$R(t) = \mathbb{E} \left[(G_{s+t} - G_s)^2 \right] = 2 \|g\|_{L^2(\mathbb{R}^+)}^2 (1 - r(t)), \quad t \geq 0.$$

We assume that the process X is observed at equidistant time points $t_i = i\Delta_n$, $i = 0, 1, \dots, \lfloor t/\Delta_n \rfloor$, with $\Delta_n \downarrow 0$ as $n \rightarrow \infty$. This kind of asymptotics is termed *in-fill asymptotics*. The theory considered in this paper will call for computing second order differences of the \mathcal{BSS} process using different lag spacing, $v \in \mathbb{N}$. In particular, we are concerned with power variations of the following type

$$V(X; p, v)_t^n \equiv \sum_{i=2v}^{\lfloor t/\Delta_n \rfloor} |X_{i\Delta_n} - 2X_{(i-v)\Delta_n} + X_{(i-2v)\Delta_n}|^p, \quad (3)$$

where $p \geq 1$ and where we refer to v as the lag between observations. Although the theory goes through for general $v \in \mathbb{N}$ we will mainly consider $v = 1, 2$, which will be sufficient for our purposes. For the asymptotic theory, [Corcuera et al. \(2013\)](#) also introduce the normalized power variations:

$$\bar{V}(X; p, v)_t^n \equiv \Delta_n \tau_n(v)^{-p} V(X; p, v)_t^n, \quad (4)$$

where $\tau_n(v) = \sqrt{\mathbb{E} \left[\left| G_{i\Delta_n} - 2G_{(i-v)\Delta_n} + G_{(i-2v)\Delta_n} \right|^2 \right]}$ is the standard deviation of the second order increment of the Gaussian core calculated with lag spacing $v\Delta_n$.

Our proposal is to use the bootstrap to approximate the sampling distributions of a general class of nonlinear transformations of these statistics. This relates to the limiting behavior of the roughness parameter estimator of the \mathcal{BSS} process, studied in [Corcuera et al. \(2013\)](#). In order to recall the consistency result for $\bar{V}(X; p, v)_t^n$, derived by [Corcuera et al. \(2013\)](#), we need to introduce a set of assumptions. Below, α denotes a number in $(-\frac{1}{2}, 0) \cup (0, \frac{1}{2})$ and functions L_f indexed by a mapping f , are assumed to be slowly varying at zero, i.e. be such that $\lim_{x \downarrow 0} \frac{L_f(tx)}{L_f(x)} = 1$ for all $t > 0$. For a function f , $f^{(k)}$ denotes the k -th derivative of f .

Assumption 1.

- (i) $g(x) = x^\alpha L_g(x)$.
- (ii) $g^{(2)}(x) = x^{\alpha-2} L_{g^{(2)}}(x)$ and for any $\epsilon > 0$, we have $g^{(2)} \in L^2((\epsilon, \infty))$. Furthermore, $|g^{(2)}|$ is non-increasing on the interval (a, ∞) for some $a > 0$.
- (iii) For any $t > 0$

$$F_t = \int_1^\infty \left| g^{(2)}(s) \right|^2 \sigma_{t-s}^2 ds < \infty$$

almost surely.

The next set of assumptions deals with the variogram R .

Assumption 2. For the roughness parameter α from Assumption 1, it holds that

- (i) $R(x) = x^{2\alpha+1} L_R(x)$.
- (ii) $R^{(4)}(x) = x^{2\alpha-3} L_{R^{(4)}}(x)$.
- (iii) There exists a $b \in (0, 1)$ such that

$$\limsup_{x \downarrow 0} \sup_{y \in [x, x^b]} \left| \frac{L_{R^{(4)}}(y)}{L_R(x)} \right| < \infty.$$

Finally, we introduce an assumption on the smoothness of the process σ .

Assumption 3. For any $q > 0$, it holds that

$$\mathbb{E} [|\sigma_t - \sigma_s|^q] \leq C_q |t - s|^{\gamma q}$$

for some $\gamma > 1/2$ and $C_q > 0$.

Remark 1 *The methods and results presented in this paper can be trivially extended to processes of the form*

$$X_t^\sharp = \int_{-\infty}^t (g(t-s) - g_0(-s)) \sigma_s dW_s, \quad t \geq 0,$$

where g is as before and $g_0 : \mathbb{R} \rightarrow \mathbb{R}$ is a measurable function such that $g(x) = 0$ for all $x < 0$ and

$$\int_{-\infty}^t (g(t-s) - g_0(-s))^2 \sigma_s^2 ds < \infty, \quad \text{for all } t \geq 0.$$

In particular, we note that $X_t^\sharp - X_s^\sharp = X_t - X_s$ for any $t > s \geq 0$, which is why the techniques that rely on the increments of X presented below, apply, *mutatis mutandis*, to X^\sharp as well.

2.2 Power variation of the BSS process and its asymptotic theory

Under Assumptions 1 and 2, Corcuera et al. (2013, Theorem 3.1 and equation (4.5)) show that for $v \in \mathbb{N}$

$$\bar{V}(X; p, v)_t^n \xrightarrow{u.c.p.} V(X; p)_t = m_p \int_0^t |\sigma_s|^p ds, \quad (5)$$

where $m_p \equiv \mathbb{E}[|U|^p]$, $U \sim N(0, 1)$, and $\xrightarrow{u.c.p.}$ denotes uniform convergence in \mathbb{P} -probability on compact sets. Corcuera et al. (2013, Theorems 3.2 and 4.5) also derive a joint asymptotic distribution of the vector $\Delta_n^{-1/2} (\bar{V}(X; p, 1)_t^n - V(X; p)_t, \bar{V}(X; p, 2)_t^n - V(X; p)_t)$. In particular, under Assumptions 1–3 (Corcuera et al., 2013, Theorem 3.2),

$$\Delta_n^{-1/2} \begin{pmatrix} \bar{V}(X; p, 1)_t^n - m_p \int_0^t |\sigma_s|^p ds \\ \bar{V}(X; p, 2)_t^n - m_p \int_0^t |\sigma_s|^p ds \end{pmatrix} \xrightarrow{st} N(0, \Sigma_{p,t}), \quad (6)$$

where \xrightarrow{st} denotes stable convergence, and

$$\Sigma_{p,t} \equiv \Lambda_p \int_0^t |\sigma_s|^{2p} ds,$$

with the matrix $\Lambda_p = (\lambda_p^{ij})_{1 \leq i, j \leq 2}$ given by

$$\begin{aligned} \lambda_p^{11} &= \lim_{n \rightarrow \infty} \Delta_n^{-1} \text{var} \left(\bar{V}(B^H; p, 1)_1^n \right), & \lambda_p^{22} &= \lim_{n \rightarrow \infty} \Delta_n^{-1} \text{var} \left(\bar{V}(B^H; p, 2)_1^n \right), \\ \lambda_p^{12} &= \lim_{n \rightarrow \infty} \Delta_n^{-1} \text{cov} \left(\bar{V}(B^H; p, 1)_1^n, \bar{V}(B^H; p, 2)_1^n \right), \end{aligned}$$

with B^H being a fractional Brownian motion with Hurst parameter $H = \alpha + 1/2$.¹ Note that the computation of the statistic $\bar{V}(X; p, v)_t^n$ requires knowledge of the factor $\tau_n(v)$, which is infeasible since it depends, among other things, on the roughness parameter α of the BSS process X .² Based on (5) and (6) Corcuera et al. (2013) construct consistent and asymptotically normal estimators of

¹Expressions for λ_p^{ij} can be found in Appendix B.

²This approach can be made feasible by first estimating the factor $\tau_n(v)$, see Barndorff-Nielsen et al. (2014, Appendix B). However, this procedure has the shortcoming that the central limit theorem no longer holds.

the roughness parameter α . Under Assumptions 1 and 2, [Corcuera et al. \(2013, equations 4.2 and 4.5\)](#) show that

$$\widehat{\alpha}(p)_t^n = h_p(\text{COF}(p)_t^n) \xrightarrow{u.c.p.} \alpha, \quad (7)$$

where

$$h_p(x) = \frac{\log_2(x)}{p} - \frac{1}{2}, \quad x > 0, \quad (8)$$

with \log_2 standing for the base-2 logarithm, whereas

$$\text{COF}(p)_t^n = \frac{V(X; p, 2)_t^n}{V(X; p, 1)_t^n}. \quad (9)$$

By the delta method and the properties of stable convergence, [Corcuera et al. \(2013, Propositions 4.2 and 4.6\)](#) deduce a feasible CLT for the roughness parameter α . Assume that the conditions of the CLT result (6), with $\alpha \in (-\frac{1}{2}, 0) \cup (0, \frac{1}{4})$ then for any $p \geq 2$, we have

$$\frac{p \log(2) V(X; p, 1)_t^n (\widehat{\alpha}(p)_t^n - \alpha)}{\sqrt{m_{2p}^{-1} V(X; 2p, 1)_t^n (-1, 1) \Lambda_p (-1, 1)^T}} \xrightarrow{d} N(0, 1). \quad (10)$$

As mentioned in the introduction, the CLT (10) may break down when $\alpha \in [\frac{1}{4}, \frac{1}{2})$. This motivated [Corcuera et al. \(2013\)](#) to develop a modified estimator implementing gaps between increments, from which the power variation (3) is computed. By letting the gaps widen sufficiently fast, the estimator satisfies a CLT and the relevant increments become asymptotically independent. In this case, one can develop a bootstrap method based on the idea of wild bootstrap. While we have also worked out the details of this approach, we relegate them to a web appendix ([Bennedsen et al., 2017](#)) for two reasons: Firstly, the case $\alpha \in [\frac{1}{4}, \frac{1}{2})$ seems to be of limited practical interest. Secondly, the theoretical results below show that the local fractional bootstrap method developed in this paper is valid for the whole range $\alpha \in (-\frac{1}{2}, \frac{1}{2})$.

The results of [Corcuera et al. \(2013\)](#) do not explicitly allow for $\alpha = 0$. However, we can show that under slightly amended assumptions, the LLN and CLT developed for the COF estimator remain valid also in this case. Indeed, only Assumptions 1(ii) and 2(ii) need to be changed. In the rest of this paper, when $\alpha = 0$, we thus work under Assumptions 1–3 above with the following modifications to 1(ii) and 2(ii):

Assumption 1.

- (ii') $g^{(2)}(x) = L_{g^{(2)}}(x)$ and for any $\epsilon > 0$, we have $g^{(2)} \in L^2((\epsilon, \infty))$. Furthermore, $|g^{(2)}|$ is non-increasing on the interval (a, ∞) for some $a > 0$.

Assumption 2.

(ii') $R^{(4)}(x) = f(x)L_{R^{(4)}}(x)$, where the function f is such that $|f(x)| \leq Cx^{-\beta}$ for some constants $C > 0$ and $\beta > 1/2$.

We now obtain the following result, which is proved in Appendix C.

Proposition 2.1 *Suppose Assumptions 1–3 hold. Then the LLN (7) and CLT (10) hold with $\alpha = 0$.*

Example 2.1 *The Ornstein-Uhlenbeck kernel $g(x) = e^{-\lambda x}$, $\lambda > 0$, satisfies Assumptions 1 and 2 with $\alpha = 0$. Indeed, Assumption 1 is trivially seen to hold and since*

$$R(x) = \lambda^{-1} \left(1 - e^{-\lambda x} \right) = xL_R(x),$$

where

$$L_R(x) = x^{-1}\lambda^{-1} \left(1 - e^{-\lambda x} \right)$$

is a slowly varying function, Assumption 2(i) also holds. We also have

$$R^{(m)}(x) = (-1)^{m-1}\lambda^{m-1}e^{-\lambda x}, \quad m \geq 1,$$

so Assumption 2(ii') holds with $f(x) = e^{-\lambda x}$ and $L_{R^{(4)}} = -\lambda^{-3}$. Lastly,

$$\lim_{x \downarrow 0} L_R(x) = 1,$$

so Assumption 2(iii) clearly also holds.

3 The local fractional bootstrap

In this section, we introduce a bootstrap method for a general class of nonlinear transformations of the vector $(\bar{V}(X; p, 1)_t^n, \bar{V}(X; p, 2)_t^n)$. We then use the method to approximate the sampling distribution of the roughness parameter estimator $\hat{\alpha}(p)_t^n$. In particular, we consider a hypothesis test where the null hypothesis is

$$H_0 : \alpha = \alpha_0$$

for some $\alpha_0 \in (-\frac{1}{2}, \frac{1}{2})$, whereas the alternative hypothesis is

$$H_1 : \alpha \neq \alpha_0.$$

Our idea is to resample the high frequency second order differences of the BSS process X as defined in (3). To be valid, the method should mimic the dependence properties of the increments of X . As pointed out in Corcuera et al. (2013), under Assumption 2, the short-term behavior of

the Gaussian core G is similar to that of a fractional Brownian motion B^H with Hurst parameter $H = \alpha + 1/2$. More precisely, for any $t_0 \in \mathbb{R}$,

$$\left(\frac{G_{\varepsilon t+t_0} - G_{t_0}}{\sqrt{\text{Var}(G_\varepsilon - G_0)}} \right)_{t \geq 0} \xrightarrow{d} (B_t^H)_{t \geq 0} \quad \text{in } C(\mathbb{R}^+)$$

as $\varepsilon \rightarrow 0$.

Consider for now the following constant-volatility toy model,

$$\tilde{X}_t = \sigma G_t = \sigma \int_{-\infty}^t g(t-s) dW_s, \quad t \geq 0, \quad (11)$$

obtained from X by setting $\sigma_t = \sigma > 0$ for all $t \in \mathbb{R}$. The above discussion suggests that in the context of \tilde{X} , the bootstrap scheme should be able to replicate the correlation structure of the increments of a fractional Brownian motion with Hurst parameter $H = \alpha + 1/2$. To this end, we propose the following local fractional bootstrap algorithm:

Step 1. Specify a null hypothesis $H_0 : \alpha = \alpha_0$ by fixing $\alpha_0 \in (-\frac{1}{2}, \frac{1}{2})$.

Step 2. Generate $\lfloor t/\Delta_n \rfloor$ random variables, $B_{\Delta_n}^H, \dots, B_{\lfloor t/\Delta_n \rfloor}^H$, which are independent of the original process X , where B^H is a fractional Brownian motion with Hurst parameter $H = \alpha_0 + 1/2$.

Step 3. Finally, return the observations

$$X_{i\Delta_n}^* = \hat{\sigma} \cdot B_{i\Delta_n}^H, \quad i = 2v, \dots, \lfloor t/\Delta_n \rfloor, \quad (12)$$

where $\hat{\sigma} = \hat{\sigma}(p, v)^n$ is a consistent estimator of the volatility σ .

This bootstrap algorithm deserves a few comments. First, we generate the bootstrap observations under the null hypothesis $H_0 : \alpha = \alpha_0$; this feature is not only natural, but it is important to minimize the probability of a type I error, see e.g. [Davidson and MacKinnon \(1999\)](#). Second, although (12) is motivated by the very simple model (11), as we will show below, this does not prevent the bootstrap method to be valid more generally. In particular, its validity extends to the case where the volatility is not constant as in (1). The choice of $\hat{\sigma}$ may change depending on the statistics of interest. As we will see shortly, for instance, when we consider the vector $\Delta_n^{-1/2} (\bar{V}(X; p, 1)_t^n, \bar{V}(X; p, 2)_t^n)$, one could simply use $\hat{\sigma} = \hat{\sigma}(p, v)_t^n = (m_p^{-1} \bar{V}(X; p, v)_t^n)^{1/p}$, cf. Equation (5).

Define the bootstrap power variations analogues of (3) and (4), respectively, as follows

$$V^*(X, B^H; p, v)_t^n \equiv \frac{|\hat{\sigma}(p, v)_t^n|^p}{\bar{\mu}(p, v)_t^n} V(B^H; p, v)_t^n, \quad (13)$$

$$\begin{aligned} \bar{V}^*(X, B^H; p, v)_t^n &\equiv \Delta_n \tau_n(v)^{-p} V^*(X, B^H; p, v)_t^n \\ &= \frac{|\hat{\sigma}(p, v)_t^n|^p}{\bar{\mu}(p, v)_t^n} \bar{V}(B^H; p, v)_t^n, \end{aligned} \quad (14)$$

where $\bar{\mu}(p, v)_t^n = \Delta_n \tau_n(v)^{-p} \mu(p, v)_t^n$ with $\mu(p, v)_t^n = \mathbb{E}^*(V(B^H; p, v)_t^n)$.

Lemma 3.1 Consider (1), (13), and (14) where B^H is a fractional Brownian motion with Hurst parameter $H = \alpha_0 + 1/2$. It follows that

- (i) $\mathbb{E}^* (\bar{V}^* (X, B^H; p, v)_t^n) = |\hat{\sigma}(p, v)_t^n|^p$.
- (ii) $Var^* \left(\Delta_n^{-1/2} \bar{V}^* (X, B^H; p, 1)_t^n \right) = \underbrace{\Delta_n^{-1} Var \left(\bar{V} (B^H; p, 1)_t^n \right)}_{\equiv \lambda_{p,n}^{11}} \frac{|\hat{\sigma}(p, 1)_t^n|^{2p}}{(\bar{\mu}(p, 1)_t^n)^2}$,
- (iii) $Var^* \left(\Delta_n^{-1/2} \bar{V}^* (X, B^H; p, 2)_t^n \right) = \underbrace{\Delta_n^{-1} Var \left(\bar{V} (B^H; p, 2)_t^n \right)}_{\equiv \lambda_{p,n}^{22}} \frac{|\hat{\sigma}(p, 2)_t^n|^{2p}}{(\bar{\mu}(p, 2)_t^n)^2}$,
- (iv) $Cov^* \left(\Delta_n^{-1/2} \bar{V}^* (X, B^H; p, 1)_t^n, \Delta_n^{-1/2} \bar{V}^* (X, B^H; p, 2)_t^n \right) = \underbrace{\Delta_n^{-1} Cov \left(\bar{V} (B^H; p, 1)_t^n, \bar{V} (B^H; p, 2)_t^n \right)}_{\equiv \lambda_{p,n}^{12}} \frac{|\hat{\sigma}(p, 1)_t^n|^p |\hat{\sigma}(p, 2)_t^n|^p}{\bar{\mu}(p, 1)_t^n \bar{\mu}(p, 2)_t^n}$,
- (v) If $|\hat{\sigma}(p, v)_t^n|^{2p} \xrightarrow{u.c.p.} \int_0^t |\sigma_s|^{2p} ds$ and $|\hat{\sigma}(p, 1)_t^n|^p |\hat{\sigma}(p, 2)_t^n|^p \xrightarrow{u.c.p.} \int_0^t |\sigma_s|^{2p} ds$, then

$$p \lim_{n \rightarrow \infty} \Sigma^* (X, B^H; p)_t^n - \tilde{\Sigma}_{p,t}^n = 0,$$

where

$$\begin{aligned} \Sigma^* (X, B^H; p)_t^n &\equiv Var^* \left(\Delta_n^{-1/2} \begin{pmatrix} \bar{V}^* (X, B^H; p, 1)_t^n \\ \bar{V}^* (X, B^H; p, 2)_t^n \end{pmatrix} \right), \text{ and} \\ \tilde{\Sigma}_{p,t}^n &\equiv \Lambda_{p,t}^n \int_0^t |\sigma_s|^{2p} ds, \end{aligned}$$

such that

$$\Lambda_{p,t}^n = \begin{pmatrix} (\bar{\mu}(p, 1)_t^n)^{-2} \lambda_{p,n}^{11} & (\bar{\mu}(p, 1)_t^n)^{-1} (\bar{\mu}(p, 2)_t^n)^{-1} \lambda_{p,n}^{12} \\ (\bar{\mu}(p, 2)_t^n)^{-1} (\bar{\mu}(p, 2)_t^n)^{-1} \lambda_{p,n}^{12} & (\bar{\mu}(p, 2)_t^n)^{-2} \lambda_{p,n}^{22} \end{pmatrix}.$$

Part (v) of Lemma 3.1 shows that the bootstrap variance $\Sigma^* (X, B^H; p)_t^n$ will only be a consistent estimator of $\Sigma_{p,t}$ under the general model (1) if the following three conditions hold true:

$$|\hat{\sigma}(p, v)_t^n|^{2p} \xrightarrow{u.c.p.} \int_0^t |\sigma_s|^{2p} ds, \quad |\hat{\sigma}(p, 1)_t^n|^p |\hat{\sigma}(p, 2)_t^n|^p \xrightarrow{u.c.p.} \int_0^t |\sigma_s|^{2p} ds \quad (15)$$

and

$$\Lambda_{p,t}^n \rightarrow \Lambda_p \quad (\text{i.e. } \bar{\mu}(p, v)_t^n \rightarrow 1). \quad (16)$$

It is easy to see that letting $\hat{\sigma}(p, v)_t^n = \left(m_{2p}^{-1} \bar{V} (X; 2p, v)_t^n \right)^{1/2p}$ will satisfy (15). However, it may not be possible to satisfy (16). For instance, for $p = 2$ (which is the most important case in practice), one can show that (see Appendix B)

$$\mu(2, 1)_t^n = (\lfloor t/\Delta_n \rfloor - 1) \Delta_n^{2H} (4 - 2^{2H}).$$

However, despite $\Sigma^*(X, B^H; p)_t^n$ not being consistent for $\Sigma_{p,t}$, we can still achieve an asymptotically valid bootstrap for the studentized distribution. To this end, we need to find a consistent estimator of $\Sigma^*(X, B^H; p)_t^n$ based on bootstrap observations. In the following, without loss of generality, we will use both choices of $\widehat{\sigma}(p, v)_t^n$ given by

$$\widehat{\sigma}(p, v)_t^n = (m_p^{-1} \bar{V}(X; p, v)_t^n)^{1/p}, \text{ for } p = 1, 2, \dots, \text{ and } v = 1, 2 \quad (17)$$

and

$$\widehat{\sigma}(p, v)_t^n = \left(m_p^{-1} \bar{V}(X; \beta p, v)_t^n \right)^{1/\beta p}, \text{ for } \beta > 0, p = 1, 2, \dots, \text{ and } v = 1, 2. \quad (18)$$

We propose the following consistent estimator of $\Sigma^*(X, B^H; p)_t^n$ defined by

$$\widehat{\Sigma}^*(X, B^H; p)_t^n = \begin{pmatrix} \lambda_{p,n}^{11} \frac{|\widehat{\sigma}(p,1)_t^{n*}|^{2p}}{(\bar{\mu}(p,1)_t^n)^2} & \lambda_{p,n}^{12} \frac{|\widehat{\sigma}(p,1)_t^{n*}|^p |\widehat{\sigma}(p,2)_t^{n*}|^p}{\bar{\mu}(p,1)_t^n \bar{\mu}(p,2)_t^n} \\ \lambda_{p,n}^{12} \frac{|\widehat{\sigma}(p,1)_t^{n*}|^p |\widehat{\sigma}(p,2)_t^{n*}|^p}{\bar{\mu}(p,1)_t^n \bar{\mu}(p,2)_t^n} & \lambda_{p,n}^{22} \frac{|\widehat{\sigma}(p,2)_t^{n*}|^{2p}}{(\bar{\mu}(p,2)_t^n)^2} \end{pmatrix} \quad (19)$$

where

$$|\widehat{\sigma}(p, v)_t^{n*}|^p = \bar{V}^*(X, B^H; p, v)_t^n. \quad (20)$$

Theorem 3.1 *Suppose that Assumptions 1–3 hold for $\alpha \in (-\frac{1}{2}, \frac{1}{2})$. Assume that bootstrap observations are given by (12) where B^H is a fractional Brownian motion with Hurst parameter $H = \alpha_0 + 1/2$. It follows that as $n \rightarrow \infty$,*

$$\begin{aligned} \widehat{\Sigma}_n^* &= \left(\widehat{\Sigma}^*(X, B^H; p)_t^n \right)^{-1/2} \Delta_n^{-1/2} \begin{pmatrix} \bar{V}^*(X, B^H; p, 1)_t^n - \mathbb{E}^*(\bar{V}^*(X, B^H; p, 1)_t^n) \\ \bar{V}^*(X, B^H; p, 2)_t^n - \mathbb{E}^*(\bar{V}^*(X, B^H; p, 2)_t^n) \end{pmatrix} \\ &\xrightarrow{d^*} N(0, I_2), \end{aligned}$$

in prob- \mathbb{P} .

Thus, we can deduce a bootstrap CLT result for the bootstrap smoothness parameter estimator $\widehat{\alpha}^*(p)_t^n$ analogue of $\widehat{\alpha}(p)_t^n$. To this end, let

$$\widehat{\alpha}^*(p)_t^n = h_p(COF^*(p)_t^n),$$

where $h_p(\cdot)$ is defined by (8), whereas

$$COF^*(p)_t^n = \frac{V^*(X, B^H; p, 2)_t^n}{V^*(X, B^H; p, 1)_t^n}. \quad (21)$$

To understand the asymptotic behavior of $COF^*(p)_t^n$, we can write

$$COF^*(p)_t^n = \left(\frac{\tau_n(2)^2}{\tau_n(1)^2} \right)^{p/2} \frac{\bar{V}^*(X, B^H; p, 2)_t^n}{\bar{V}^*(X, B^H; p, 1)_t^n}.$$

From Assumption 2, we have

$$\left(\frac{\tau_n(2)^2}{\tau_n(1)^2} \right)^{p/2} \rightarrow 2^{\frac{(2\alpha+1)p}{2}},$$

and thus by Theorem 3.1, part (i) of Lemma 3.1, in conjunction with (17) and (18), and by using equation (5) with $v = 1, 2$, we can deduce that

$$\frac{\bar{V}^*(X, B^H; p, 2)_t^n}{\bar{V}^*(X, B^H; p, 1)_t^n} \xrightarrow{\mathbb{P}^*} 1, \quad \text{in prob-}\mathbb{P}.$$

It follows that, by applying the delta method on the CLT results of Theorem 3.1, we can characterize the distribution of $\hat{\alpha}^*(p)_t^n$. These results are summarized in the following theorem.

Theorem 3.2 *Suppose that Assumptions 1–3 hold for $\alpha \in (-\frac{1}{2}, \frac{1}{2})$. Assume that bootstrap observations are given by (12) where B^H is a fractional Brownian motion with Hurst parameter $H = \alpha_0 + 1/2$. It follows that for any $p \geq 2$, as $n \rightarrow \infty$,*

$$T_{\hat{\alpha}, n}^* \equiv \Delta_n^{-1/2} \frac{(\hat{\alpha}^*(p)_t^n - \tilde{\alpha}(p)_t^n)}{\sqrt{\hat{V}^*(\hat{\alpha})_t}} \xrightarrow{d^*} N(0, 1), \quad \text{in prob-}\mathbb{P},$$

where

$$\tilde{\alpha}(p)_t^n = h_p \left(\widetilde{COF}(p)_t^n \right), \quad (22)$$

such that

$$\begin{aligned} \widetilde{COF}(p)_t^n &= \left(\frac{\tau_n(2)^2}{\tau_n(1)^2} \right)^{p/2} \frac{|\hat{\sigma}(p, 2)_t^n|^p}{|\hat{\sigma}(p, 1)_t^n|^p} \\ &= \begin{cases} \frac{V(X; p, 2)_t^n}{V(X; p, 1)_t^n}, & \text{if } \hat{\sigma}(p, v)_t^n \text{ is given by (17),} \\ \left(\frac{V(X; \beta p, 2)_t^n}{V(X; \beta p, 1)_t^n} \right)^{1/\beta}, & \text{if } \hat{\sigma}(p, v)_t^n \text{ is given by (18),} \end{cases} \end{aligned}$$

and the estimator of the asymptotic variance $\hat{V}^*(\hat{\alpha})_t$ is defined as

$$\hat{V}^*(\hat{\alpha})_t = \frac{1}{(p \log(2))^2} \hat{\varsigma}^*(X, B^H; p)_t^n, \quad (23)$$

with

$$\begin{aligned} \hat{\varsigma}^*(X, B^H; p)_t^n &= \frac{\lambda_{p,n}^{11}}{[\mathbb{E}^*(\bar{V}^*(X, B^H; p, 1)_t^n)]^2} \frac{(|\hat{\sigma}(p, 1)_t^{n*}|^p)^2}{(\bar{\mu}(p, 1)_t^n)^2} + \frac{\lambda_{p,n}^{22}}{[\mathbb{E}^*(\bar{V}^*(X, B^H; p, 2)_t^n)]^2} \frac{(|\hat{\sigma}(p, 2)_t^{n*}|^p)^2}{(\bar{\mu}(p, 2)_t^n)^2} \\ &\quad - 2 \frac{\lambda_{p,n}^{12}}{\mathbb{E}^*(\bar{V}^*(X, B^H; p, 1)_t^n) \mathbb{E}^*(\bar{V}^*(X, B^H; p, 2)_t^n)} \frac{|\hat{\sigma}(p, 1)_t^{n*}|^p |\hat{\sigma}(p, 2)_t^{n*}|^p}{\bar{\mu}(p, 1)_t^n \bar{\mu}(p, 2)_t^n}. \end{aligned}$$

Remark 2 *Note that the bootstrap statistic $T_{\hat{\alpha}, n}^*$ is feasible: it is only a function of the original sample of the observed data $\{X_{i\Delta_n}\}$, the fractional Brownian motion generated in Step 2, $\{B_{i\Delta_n}^H\}$,*

and their absolute moments $\left\{E \left| B_{i\Delta_n}^H - 2B_{(i-v)\Delta_n}^H + B_{(i-2v)\Delta_n}^H \right|^p \right\}$. To see this, write

$$\hat{\alpha}^*(p)_t^n = h_p(COF^*(p)_t^n),$$

where $h_p(\cdot)$ and $COF^*(p)_t^n$ are given in (8) and (21), respectively. Given (21) and (13), it follows that

$$\begin{aligned} COF^*(p)_t^n &= \left(\frac{\tau_n(2)^2}{\tau_n(1)^2} \right)^{p/2} \frac{\bar{V}^*(X, B^H; p, 2)_t^n}{\bar{V}^*(X, B^H; p, 1)_t^n} \\ &= \begin{cases} \frac{\mu(p,1)_t^n V(B^H;p,2)_t^n V(X;p,2)_t^n}{\mu(p,2)_t^n V(B^H;p,1)_t^n V(X;p,1)_t^n}, & \text{if } \hat{\sigma}(p, v)_t^n \text{ is given by (17),} \\ \frac{\mu(p,1)_t^n V(B^H;p,2)_t^n}{\mu(p,2)_t^n V(B^H;p,1)_t^n} \left(\frac{V(X;\beta p, 2)_t^n}{V(X;\beta p, 1)_t^n} \right)^{1/\beta}, & \text{if } \hat{\sigma}(p, v)_t^n \text{ is given by (18).} \end{cases} \end{aligned} \quad (24)$$

Similarly, when $\hat{\sigma}(p, v)_t^n$ is given by (17) or (18), we can write $\hat{V}^*(\hat{\alpha})_t$ given in Theorem 3.2 through

$$\hat{V}^*(\hat{\alpha})_t = \frac{1}{(p \log(2))^2} \hat{\zeta}^*(X, B^H; p)_t^n,$$

with

$$\hat{\zeta}^*(X, B^H; p)_t^n = A + B + C,$$

where

$$\begin{aligned} A &= \Delta_n^{-1} (\mu(p, 1)_t^n)^{-4} \left(V(B^H; p, 1)_t^n \right)^2 \text{Var} \left(V(B^H; p, 1)_t^n \right), \\ B &= \Delta_n^{-1} (\mu(p, 2)_t^n)^{-4} \left(V(B^H; p, 2)_t^n \right)^2 \text{Var} \left(V(B^H; p, 2)_t^n \right), \\ C &= C_1 \cdot C_2, \end{aligned}$$

and

$$\begin{aligned} C_1 &= -2 (\mu(p, 1)_t^n)^{-2} (\mu(p, 2)_t^n)^{-2} V(B^H; p, 1)_t^n V(B^H; p, 2)_t^n, \\ C_2 &= \Delta_n^{-1} \text{Cov} \left(V(B^H; p, 1)_t^n, V(B^H; p, 2)_t^n \right). \end{aligned}$$

Expressions for $\text{Var} \left(V(B^H; p, v)_t^n \right)$, $\text{Cov} \left(V(B^H; p, 1)_t^n, V(B^H; p, 2)_t^n \right)$ and $\mu(p, v)$ for $p = 2$ can be found in Appendix B.

3.1 Bootstrap implementation

We can use the bootstrap method proposed above to test hypotheses on the roughness of the sample paths of a \mathcal{BSS} process. Consider the following, where the null hypothesis is $H_0 : \alpha = \alpha_0$ for some $\alpha_0 \in \left(-\frac{1}{2}, \frac{1}{2}\right)$, whereas the alternative hypothesis is $H_1 : \alpha \neq \alpha_0$. We let $p = 2$. For a given time period $[0, t]$ with step size $\Delta_n = \frac{t}{n}$ we suppose we have $n + 1 \in \mathbb{N}$ observations $\mathbb{X} = (X_0, X_{\Delta_n}, \dots, X_{n\Delta_n})$ of a \mathcal{BSS} process. Below, B is the number of bootstrap replications (e.g. $B = 999$).

Algorithm for hypothesis testing using the Local Fractional Bootstrap

1. From the data \mathbb{X} , compute the estimate of the roughness parameter α given by

$$\hat{\alpha}(2)_t^n = h_2(COF(2)_t^n),$$

where $h_p(\cdot)$ and $COF(2)_t^n$ are given in (8) and (9), respectively. Then, compute an estimator of the asymptotic variance $V(\hat{\alpha})_t^n = \lim_{n \rightarrow \infty} Var(\hat{\alpha}(2)_t^n)$, given by

$$\hat{V}(\hat{\alpha})_t = n \frac{m_{2p}^{-1} V(X; 4, 1)_t^n (-1, 1) \Lambda_2(-1, 1)^T}{(2 \log(2) V(X; 2, 1)_t^n)^2}.$$

2. Simulate $n + 1$ observations $B_0^H, B_{\Delta_n}^H, \dots, B_{n\Delta_n}^H$ of a fractional Brownian motion with Hurst parameter $H = \alpha_0 + 1/2$ that are independent of the data \mathbb{X} .

3. Using the simulated sample $(B_0^H, B_1^H, \dots, B_n^H)$, compute the estimate of the bootstrap roughness parameter $\hat{\alpha}^*(2)_t^n$, given by

$$\hat{\alpha}^*(2)_t^n = h_2(COF^*(2)_t^n),$$

where $h_p(\cdot)$ and $COF^*(p)_t^n$ are given in (8) and (24), respectively.

4. The actual test relies on the bootstrap studentized statistic. Thus, compute

$$T_{\hat{\alpha}, n}^* = \Delta_n^{-1/2} \frac{(\hat{\alpha}^*(2)_t^n - \tilde{\alpha}(2)_t^n)}{\sqrt{\hat{V}^*(\hat{\alpha})_t}},$$

where $\tilde{\alpha}(2)_t^n$ is given by (22), whereas $\hat{\alpha}^*(2)_t^n$ is obtained in step 3, and $\hat{V}^*(\hat{\alpha})_t$ is defined in (23).

5. Repeat steps 2–4 B times and store the values of $T_{\hat{\alpha}, n, j}^*$, $j = 1, \dots, B$.

6. Reject $H_0 : \alpha = \alpha_0$, when

$$\alpha_0 \notin IC_{perc-t, 1-\gamma}^* = \left[\hat{\alpha}(2)_t^n - n^{-1/2} q_{1-\gamma/2}^* \sqrt{\hat{V}(\hat{\alpha})_t}, \hat{\alpha}(2)_t^n - n^{-1/2} q_{\gamma/2}^* \sqrt{\hat{V}(\hat{\alpha})_t} \right],$$

where $q_{\gamma/2}^*$ and $q_{1-\gamma/2}^*$ are the $\gamma/2$ and $1 - \gamma/2$ quantiles of the bootstrap distribution of T_n^* , respectively.

4 Monte Carlo simulation study

In this section, we evaluate the finite sample performance of the test based on local fractional bootstrap and compare it to the performance of the CLT-based test. In our simulations we take g to be the gamma kernel, i.e. $g(x) = x^\alpha e^{-\lambda x}$ for $x > 0$ and with $\lambda = 1$. For an in-depth analysis of the theoretical properties of the gamma kernel, see Barndorff-Nielsen (2012, 2016). We consider

$\alpha \in \{-1/3, -1/6, 0, 1/6, 1/3\}$; recall that the CLT for the COF estimator does not hold when when $\alpha \in [1/4, 1/2)$. We experimented with several different values of λ and α , but the results were in all cases very similar to what we find below. We consider three specifications for the stochastic volatility process:

- constant volatility (NoSV),
- one-factor stochastic volatility (SV1F),
- two-factor stochastic volatility (SV2F).

The details of these specifications, along with the simulation procedure, are explained in Appendix A. Our investigations concern the finite sample size of the test $H_0 : \alpha = \alpha_0$ against the two-sided alternative $H_1 : \alpha \neq \alpha_0$ at (nominal) 5% level. We also calculate the *size-adjusted power* of the test at 5% level where the (now false) null hypothesis is $H_0 : \alpha = 0$.³ The null hypothesis $H_0 : \alpha = 0$ is particularly interesting as $\alpha = 0$ is a necessary condition for the semimartingality of X . Further, in the case of the gamma kernel $g(x) = x^\alpha e^{-\lambda x}$ that we consider here, $\alpha = 0$ implies that the \mathcal{BSS} process actually is an Ornstein-Uhlenbeck process.

Tables 1 and 2 contain the results of our Monte Carlo study and detail the finite sample properties of both the CLT and the local fractional bootstrap. Table 1 presents rejection rates of H_0 when H_0 is true (i.e. the size), while Table 2 displays rejection rates of H_0 when H_1 is true (i.e. the power). Some clear conclusions can be drawn. Firstly, the bootstrap method offers clear gains in the size of the test when the number of observations, n , is small. Secondly, the power of the CLT is slightly better for $\alpha < 0$, while the opposite is true for $\alpha \geq 0$. Finally, the presence or absence of SV does not alter results very much, except in the case of SV2F where the methods lose some power.

5 Empirical applications

In this section, we apply the local fractional bootstrap method presented above to two relevant empirical data sets. As we saw in the previous section, the bootstrap method is crucial for achieving the correct empirical size of the hypothesis test $H_0 : \alpha = \alpha_0$, especially when the number of observations n is small. In both of our applications, theoretical arguments suggest specific null hypotheses to be true, and we examine how the CLT and bootstrap fare in confirming or rejecting these hypotheses.

³The size-adjusted power was obtained in the following way: Using Monte Carlo simulations we found critical values that would result in the CLT obtaining the same size as the bootstrap (see Table 1 for these size numbers); these critical values were then used to determine the power of the CLT-based test. As the bootstrap test seems to be correctly sized for all n this was not size-corrected. By using the actual size of the bootstrap test (instead of the nominal 5%) to calculate the size-adjusted critical value for the CLT-based test, the power properties of the two tests become comparable.

Table 1: *Rejection rates under H_0*

Panel A: NoSV										
n	$\alpha = -1/3$		$\alpha = -1/6$		$\alpha = 0$		$\alpha = 1/6$		$\alpha = 1/3$	
	CLT	boot	CLT	boot	CLT	boot	CLT	boot	CLT	boot
20	0.0968	0.0470	0.0950	0.0454	0.0968	0.0354	0.1044	0.0478	0.1110	0.0456
40	0.0742	0.0534	0.0728	0.0540	0.0754	0.0488	0.0746	0.0584	0.0852	0.0558
80	0.0642	0.0568	0.0562	0.0512	0.0644	0.0550	0.0638	0.0526	0.0726	0.0610
160	0.0620	0.0596	0.0638	0.0598	0.0536	0.0514	0.0576	0.0558	0.0572	0.0528
320	0.0568	0.0556	0.0540	0.0530	0.0562	0.0526	0.0610	0.0582	0.0548	0.0516
Panel B: SV1F										
n	$\alpha = -1/3$		$\alpha = -1/6$		$\alpha = 0$		$\alpha = 1/6$		$\alpha = 1/3$	
	CLT	boot	CLT	boot	CLT	boot	CLT	boot	CLT	boot
20	0.1012	0.0466	0.1124	0.0506	0.1052	0.0380	0.1050	0.0466	0.1222	0.0554
40	0.0740	0.0542	0.0796	0.0550	0.0772	0.0464	0.0796	0.0552	0.0872	0.0612
80	0.0580	0.0526	0.0588	0.0512	0.0652	0.0526	0.0658	0.0552	0.0686	0.0610
160	0.0614	0.0596	0.0546	0.0506	0.0584	0.0558	0.0622	0.0572	0.0660	0.0590
320	0.0564	0.0558	0.0508	0.0546	0.0502	0.0492	0.0532	0.0536	0.0528	0.0512
Panel C: SV2F										
n	$\alpha = -1/3$		$\alpha = -1/6$		$\alpha = 0$		$\alpha = 1/6$		$\alpha = 1/3$	
	CLT	boot	CLT	boot	CLT	boot	CLT	boot	CLT	boot
20	0.0918	0.0400	0.0962	0.0470	0.0986	0.0340	0.1092	0.0516	0.1458	0.0534
40	0.0734	0.0548	0.0638	0.0504	0.0748	0.0516	0.0822	0.0670	0.1056	0.0634
80	0.0616	0.0584	0.0656	0.0624	0.0686	0.0572	0.0678	0.0620	0.0844	0.0632
160	0.0558	0.0544	0.0612	0.0594	0.0572	0.0550	0.0630	0.0606	0.0650	0.0602
320	0.0562	0.0562	0.0572	0.0554	0.0512	0.0508	0.0550	0.0574	0.0624	0.0602

Simulation study of the finite sample properties of the test $H_0 : \alpha = \alpha_0$ against the alternative $H_1 : \alpha \neq \alpha_0$, using the CLT and the local fractional bootstrap. The simulations are done under H_0 , i.e. we consider the size of the tests. The nominal size is 5% and the numbers shown are the rejection rates of H_0 over 5 000 Monte Carlo simulations, each with $B = 999$ bootstrap replications. We set $p = 2$ and $\lambda = 1$.

Table 2: *Rejection rates under H_1*

Panel A: NoSV								
n	$\alpha = -1/3$		$\alpha = -1/6$		$\alpha = 1/6$		$\alpha = 1/3$	
	CLT	boot	CLT	boot	CLT	boot	CLT	boot
20	0.2308	0.1566	0.1010	0.0708	0.0244	0.0510	0.0284	0.1118
40	0.3792	0.2886	0.1646	0.1148	0.0572	0.1030	0.1820	0.3146
80	0.6168	0.5428	0.2356	0.1848	0.1314	0.1994	0.5342	0.6212
160	0.8688	0.8248	0.3874	0.3228	0.2990	0.3526	0.8660	0.8998
320	0.9918	0.9852	0.6160	0.5654	0.5722	0.6074	0.9920	0.9964
Panel B: SV1F								
n	$\alpha = -1/3$		$\alpha = -1/6$		$\alpha = 1/6$		$\alpha = 1/3$	
	CLT	boot	CLT	boot	CLT	boot	CLT	boot
20	0.2182	0.1536	0.1162	0.0710	0.0214	0.0472	0.0352	0.1084
40	0.3812	0.2914	0.1644	0.1108	0.0530	0.0986	0.1850	0.3052
80	0.5834	0.5350	0.2204	0.1958	0.1376	0.1880	0.5300	0.6126
160	0.8692	0.8302	0.3652	0.3242	0.2888	0.3458	0.8674	0.9020
320	0.9890	0.9874	0.6270	0.5672	0.5598	0.6092	0.9928	0.9948
Panel C: SV2F								
n	$\alpha = -1/3$		$\alpha = -1/6$		$\alpha = 1/6$		$\alpha = 1/3$	
	CLT	boot	CLT	boot	CLT	boot	CLT	boot
20	0.1706	0.1166	0.0966	0.0628	0.0258	0.0450	0.0136	0.0686
40	0.2834	0.2238	0.1250	0.0988	0.0678	0.0948	0.0928	0.1942
80	0.4332	0.3598	0.1814	0.1312	0.1140	0.1446	0.2716	0.3740
160	0.6252	0.5890	0.2486	0.1960	0.1998	0.2338	0.5582	0.6262
320	0.8676	0.8396	0.3980	0.3468	0.3362	0.4008	0.8320	0.8620

Simulation study of the finite sample properties of the test $H_0 : \alpha = 0$ against the alternative $H_1 : \alpha \neq 0$, using the CLT and the local fractional bootstrap. The simulations are done under the alternative, i.e. we consider the power of the tests, with the true value of α used in the simulations being the α indicated in the respective column. For the bootstrap, the nominal size is 5%, while the CLT has been size-adjusted as explained in the text: the critical value used is the critical value that results in the CLT having the same size as the bootstrap test (given in Table 1). The numbers shown are the rejection rates of H_0 over 5 000 Monte Carlo simulations, each with $B = 999$ bootstrap replications. We set $p = 2$ and $\lambda = 1$.

5.1 High-frequency futures price data

Here, we consider testing $H_0 : \alpha = 0$ for the price of a financial asset, the E-mini S&P 500 futures contract. Note that, at least theoretically, on no-arbitrage grounds (Delbaen and Schachermayer, 1994, Theorem 7.2) one would expect H_0 to be true, since $\alpha \neq 0$ implies that the BSS process is not a semimartingale (e.g. Corcuera et al., 2013; Bennedsen, 2016).

Our data consists of high-frequency⁴ observations of the E-mini S&P 500 futures contract, traded on CME Globex electronic trading platform, from January 2, 2013 until December 31, 2014, excluding weekends and holidays. This results in 516 trading days, 18 of which were not full trading days; we removed these to arrive at a total of 498 days in our sample. Although the E-mini S&P 500 contract is traded almost around the clock, we restrict attention to the most liquid time period which is when the NYSE is open, i.e. to the 6.5 hours from 9.30 a.m. to 4 p.m. EST. We resample the price at different frequencies, $\Delta \in \{2, 5, 10, 15\}$ minutes, which results in $n = 196, 79, 40, 27$ daily prices, respectively. We then test $H_0 : \alpha = 0$ for each day using both the CLT and the local fractional bootstrap against the two-sided alternative $H_1 : \alpha \neq 0$. The results, averaged over the 498 days in our sample, are presented in Figure 1. We see that when we sample the price frequently ($\Delta = 2$ minutes), both methods reject often (16.5% and 14.1%, respectively) indicating that the number of days when $H_0 : \alpha = 0$ is rejected is significant. This result may seem surprising, but is likely due to market microstructure (MMS) noise effects: at very short time scales, high-frequency data often exhibits negative autocorrelations that are compatible with the alternative hypothesis $\alpha < 0$.

When sampling at lower frequencies, i.e. Δ being at least 5 minutes, one expects the MMS effects to be negligible and rejections of H_0 should occur at the nominal rate. Figure 1 indeed shows that we reject H_0 less often in these cases; we also observe that the bootstrap method rejects less often than the CLT. Indeed, the bootstrap is closer to the nominal 5% rejection rate which we would expect under H_0 . In the case $\Delta = 15$ minutes, we have only $n = 27$ observations per day; considering the Monte Carlo evidence above, we expect the CLT to be oversized in this case. As seen in the figure, the CLT indeed rejects H_0 more often here (11.4%) while the bootstrap essentially retains the nominal size, rejecting on 4.6% of the days. This is encouraging as any MMS effects should be negligible at this time scale.

5.2 Turbulence data

In our second application, we study a time series of one-dimensional hot-wire anemometer measurements of the longitudinal component of a turbulent velocity field in the atmospheric boundary layer, measured 35 meters above ground level. The time series consists of 2×10^7 observations, sampled at a rate of 5 kHz. In other words, there are 20 million observations, measured over a

⁴The data has been recorded with one-second time stamp precision.

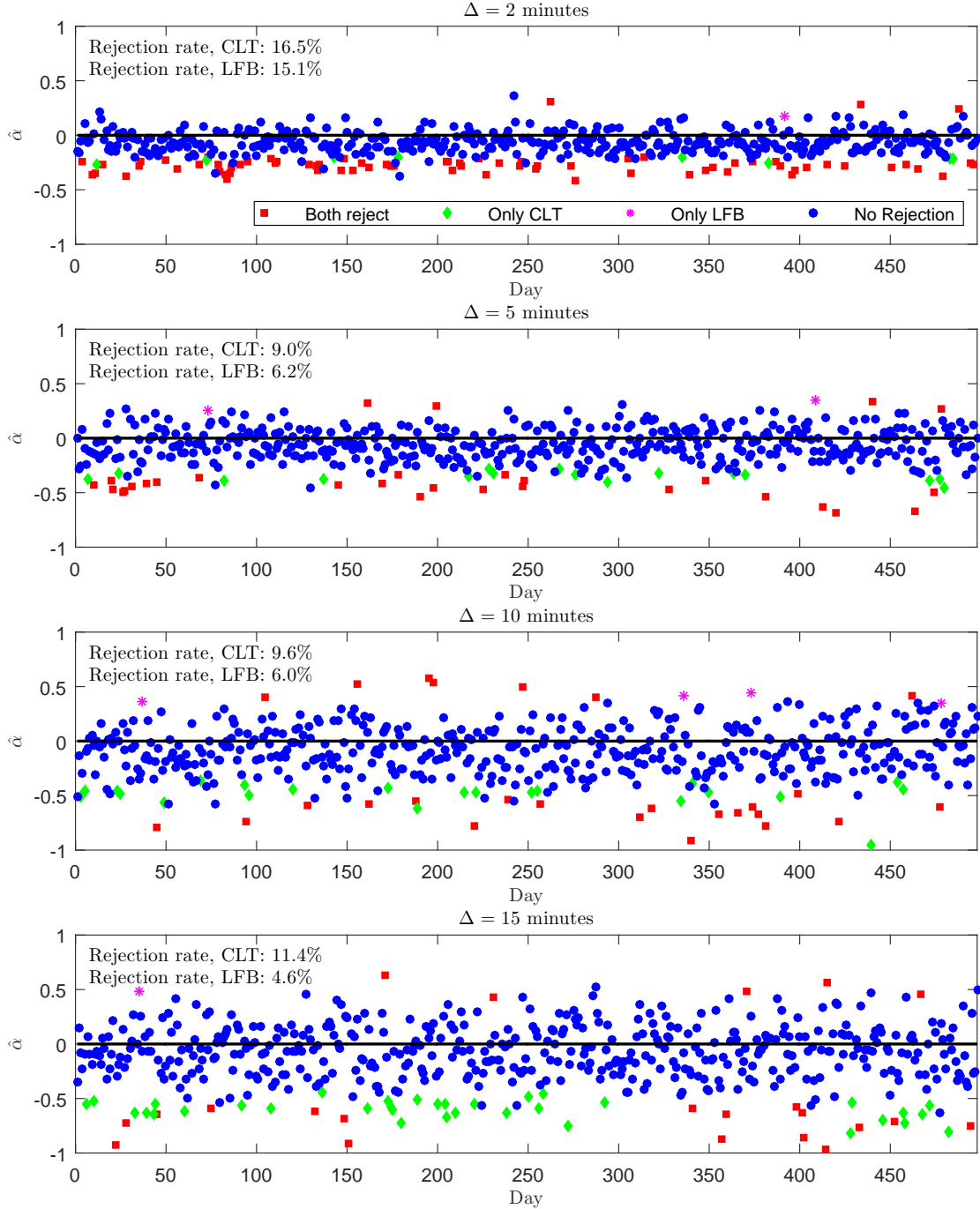


Figure 1: Estimates of α and test of $H_0 : \alpha = 0$ against $H_1 : \alpha \neq 0$ from 498 intraday time series of log-prices from the E-mini data set, sampled every Δ period. The plots depict the estimated value of α from a given day. The particular days where H_0 was rejected by both the CLT and LFB are shown by red squares; the days where only the CLT, but not the LFB, rejected are green diamonds; the days where only the LFB, but not the CLT, rejected are magenta asterisks; and the days where no method rejects H_0 are blue circles. We used $B = 999$ bootstrap replications and the black horizontal line indicates the null value $\alpha = 0$.

period of $T = 4000$ seconds with 5000 observations recorded per second. This time series was also studied in [Corcuera et al. \(2013\)](#) and [Barndorff-Nielsen et al. \(2014\)](#), and we refer to [Dhruva \(2000\)](#) for further details on how it was recorded.

When timewise data on turbulence is modeled using a \mathcal{BSS} process whose kernel function satisfies Assumption 1(i), Kolmogorov’s 5/3 scaling law ([Kolmogorov, 1941](#)) for fully developed turbulence, assuming Taylor’s frozen field hypothesis ([Taylor, 1938](#)), is compatible with the parameter value $\alpha = -1/6$ at intermediate time scales that correspond to the so-called *inertial range*; see also [Márquez and Schmiegel \(2016\)](#). By analyzing the spectral density of the time series, for this data the inertial range was found to be approximately between 0.1 Hz and 200 Hz ([Corcuera et al., 2013](#), Section 5).

As in the previous application, we experiment with resampling the data at various frequencies f , varying f to study the roughness properties of the time series at different time scales. More specifically, we vary f between 1 Hz and 200 Hz to include time scales both firmly within and on the border of the inertial range. The time increment Δ used in resampling is related to f by $\Delta = 1/f$. Motivated by Kolmogorov’s scaling law, we formulate $H_0 : \alpha = -1/6$ and test it against the two-sided alternative $H_1 : \alpha \neq -1/6$. In our analysis, we divide the sample period (of 4000 seconds) into $M = 400$ sub-periods of 10 seconds. We conduct the test on each sub-period individually, treating them as separate measurements of the same phenomenon, which seems reasonable given the putative stationarity of the time series. Note that after resampling at frequency f , the number of observations covering each sub-period is $n = 10f$.

Figure 2 presents results on the rejection rate of H_0 , which is the relative frequency of rejections over the $M = 400$ sub-periods. As expected, H_0 is often rejected when the sampling rate is on the border of the inertial range (cf. the results for $f = 200$ Hz). When firmly inside the inertial range ($f = 20$ Hz), the null hypothesis is rejected in roughly 4% of the sub-periods for both methods. At these sampling frequencies, the CLT- and bootstrap-based tests largely agree; this is as expected since there are plenty of observations.

The results change as the sampling frequency is lowered, resulting in fewer observations. Indeed, we see that the CLT-based test yields rejection rates of 10.8% and 17.3% at sampling frequencies 1 and 2 Hz, respectively, while the bootstrap-based test rejects roughly at the nominal 5% rate, as we would expect from a correctly-sized test when H_0 is true. As seen also in the previous application, at low sampling frequencies (here 1 Hz, which leads to $n = 10$ observations), the COF estimator seems to be severely biased (the mean of the estimates of α is around -0.475). In this case, the CLT-based test starts rejecting H_0 at an unplausibly high rate (around 17%) while the bootstrap-based test is more conservative with rejection rate around 6%. As we would still expect the null hypothesis $H_0 : \alpha = -1/6$ to be actually true at this sampling frequency, it is reassuring that the bootstrap-based test is so close to the nominal rate 5% in this, arguably extreme, case.

However, this comes with the caveat that $n = 10$ observations might simply be too few to draw any definite conclusion on.

6 Conclusion

We have proposed a novel bootstrap method of conducting inference on the roughness index α of a Brownian semistationary process using the change-of-frequency estimator. While our simulation study indicates that the performance of both the CLT- and bootstrap-based tests is generally good, the bootstrap approach improves the size properties of the test of $H_0 : \alpha = \alpha_0$ when the number of observations is moderate or small.

As an application, we applied the method to test for $H_0 : \alpha = 0$ with a time series of intraday prices of the E-mini S&P 500 futures contract and to test for $H_0 : \alpha = -1/6$ with a time series of measurements of atmospheric turbulence. With both data sets, we observed what the simulation results already indicated: the CLT rejects the respective null hypotheses, that we expect to be true on theoretical grounds, too often when the number of observations is limited, while the local fractional bootstrap retains the correct size. We conclude that the local fractional bootstrap is a powerful alternative to the CLT when drawing inference on the roughness index α , and it appears to be essential at lower observation frequencies.

Finally, we note that while in this paper we have focused on \mathcal{BSS} processes, the local fractional bootstrap method should be applicable to other “fractional” processes such as the fractional Brownian motion (fBm), fractional Ornstein-Uhlenbeck process, and the like. We leave such extensions for future work.

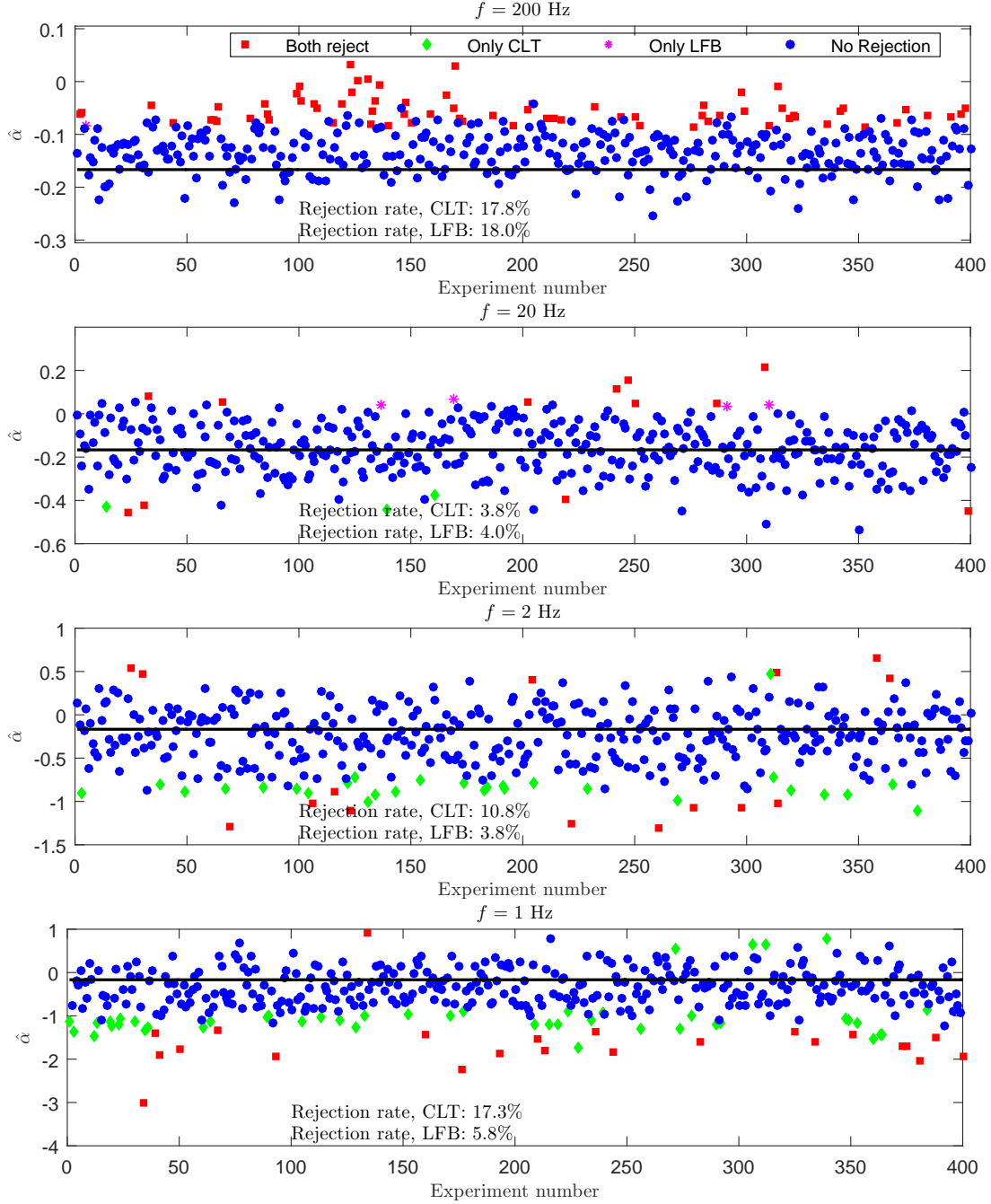


Figure 2: Estimates of α and test of $H_0 : \alpha = -1/6$ against $H_1 : \alpha \neq -1/6$ from 400 experiments using the turbulence data described in the text, see also Dhruva (2000). The data is sampled at frequency f . The plots depict the estimated value of α from a given experiment. The particular experiments where H_0 was rejected by both the CLT and LFB are shown by red squares; the experiments where only the CLT, but not the LFB, rejected are green diamonds; the experiments where only the LFB, but not the CLT, rejected are magenta asterisks; and the experiments where no method rejects H_0 are blue circles. We used $B = 999$ bootstrap replications and the black horizontal line indicates the null value $\alpha = -1/6$.

References

- Barndorff-Nielsen, O. E. (2012). Notes on the gamma kernel. Thiele Centre Research Report, No. 03, May 2012.
- Barndorff-Nielsen, O. E. (2016). Assessing Gamma kernels and BSS/LSS processes. *CREATES Working Paper 2016-09*.
- Barndorff-Nielsen, O. E., F. E. Benth, and A. E. D. Veraart (2013). Modelling energy spot prices by volatility modulated Lévy-driven Volterra processes. *Bernoulli* 19(3), 803–845.
- Barndorff-Nielsen, O. E., J. M. Corcuera, and M. Podolskij (2009). Power variation for Gaussian processes with stationary increments. *Stochastic Processes and their Applications* 119(6), 1845–1865.
- Barndorff-Nielsen, O. E., J. M. Corcuera, and M. Podolskij (2011). Multipower variation for Brownian semistationary processes. *Bernoulli* 4(17), 1159–1194.
- Barndorff-Nielsen, O. E., J. M. Corcuera, and M. Podolskij (2013). Limit theorems for functionals of higher order differences of Brownian semistationary processes. In A. N. Shiryaev, S. R. S. Varadhan, and E. Presman (Eds.), *Prokhorov and Contemporary Probability Theory*, pp. 69–96. Berlin: Springer.
- Barndorff-Nielsen, O. E., P. R. Hansen, A. Lunde, and N. Shephard (2008). Designing realized kernels to measure the ex post variation of equity prices in the presence of noise. *Econometrica* 76(6), 1481–1536.
- Barndorff-Nielsen, O. E., M. S. Pakkanen, and J. Schmiegel (2014). Assessing relative volatility/intermittency/energy dissipation. *Electronic Journal of Statistics* 8(2), 1996–2021.
- Barndorff-Nielsen, O. E. and J. Schmiegel (2007). Ambit processes: with applications to turbulence and tumour growth. In *Stochastic analysis and applications*, Volume 2 of *Abel Symposia*, pp. 93–124. Berlin: Springer.
- Barndorff-Nielsen, O. E. and J. Schmiegel (2009). Brownian semistationary processes and volatility/intermittency. In *Advanced financial modelling*, Volume 8 of *Radon Series on Computational and Applied Mathematics*, pp. 1–25. Berlin: Walter de Gruyter.
- Basse, A. (2008). Gaussian moving averages and semimartingales. *Electron. J. Probab.* 13(39), 1140–1165.
- Bennedsen, M. (2016). Semiparametric bootstrap inference on the fractal index of a time series. Working paper, available at: <https://arxiv.org/abs/1608.01895>.
- Bennedsen, M. (2017). A rough multi-factor model of electricity spot prices. *Energy Economics* 63, 301–313.
- Bennedsen, M., U. Hounyo, A. Lunde, and M. S. Pakkanen (2017). Web appendix to the local fractional bootstrap. Available at: <https://sites.google.com/site/mbennedsen/research>.
- Bennedsen, M., A. Lunde, and M. S. Pakkanen (2016). Decoupling the short- and long-term behavior of stochastic volatility. Working paper, available at: <https://arxiv.org/abs/1610.00332>.
- Bennedsen, M., A. Lunde, and M. S. Pakkanen (2017). Hybrid scheme for Brownian semistationary processes. Forthcoming in *Finance and Stochastics*.
- Breuer, P. and P. Major (1983). Central limit theorems for nonlinear functionals of gaussian fields. *Journal of Multivariate Analysis* 13(3), 425–441.
- Corcuera, J. M., E. Hedevarang, M. S. Pakkanen, and M. Podolskij (2013). Asymptotic theory for Brownian semi-stationary processes with application to turbulence. *Stochastic Processes and their Applications* 123(7), 2552–2574.

- Davidson, R. and J. G. MacKinnon (1999). The size distortion of bootstrap tests. *Econometric Theory* 15(3), 361–376.
- Delbaen, F. and W. Schachermayer (1994). A general version of the fundamental theorem of asset pricing. *Mathematische Annalen* 300(1), 463–520.
- Dhruva, B. R. (2000). *An experimental study of high Reynolds number turbulence in the atmosphere*. Ph. D. thesis, Yale University.
- Gatheral, J., T. Jaisson, and M. Rosenbaum (2014). Volatility is rough. Working paper, available at: <http://arxiv.org/abs/1410.3394>.
- Glasserman, P. (2003). *Monte Carlo Methods in Financial Engineering*. New York: Springer.
- Gneiting, T., H. Ševčíková, and D. B. Percival (2012). Estimators of fractal dimension: assessing the roughness of time series and spatial data. *Statistical Science* 27(2), 247–277.
- Gonçalves, S. and N. Meddahi (2009). Bootstrapping realized volatility. *Econometrica* 77(1), 283–306.
- Huang, X. and G. Tauchen (2005). The relative contribution of jumps to total price variation. *Journal of Financial Econometrics* 3(4), 456–499.
- Kolmogorov, A. N. (1940). Wienerische Spiralen und einige andere interessante Kurven im Hilbertschen Raum. *Comptes Rendus de l'Académie des Sciences de l'URSS* 26(2), 115–118.
- Kolmogorov, A. N. (1941). The local structure of turbulence in incompressible viscous fluid for very large Reynolds numbers. *Doklady Akademii Nauk SSSR* 30(4), 299–303.
- Lang, G. and F. Roueff (2001). Semi-parametric estimation of the Hölder exponent of a stationary Gaussian process with minimax rates. *Statistical Inference for Stochastic Processes* 4(3), 283–306.
- Liu, R. Y. (1988). Bootstrap procedure under some non-i.i.d. models. *Annals of Statistics* 16(4), 1696–1708.
- Mandelbrot, B. B. and J. W. Van Ness (1968). Fractional Brownian motions, fractional noises and applications. *SIAM Review* 10(4), 422–437.
- Márquez, J. U. and J. Schmiegel (2016). Modelling turbulent time series by BSS-processes. In M. Podolskij, R. Stelzer, S. Thorbjørnsen, and A. E. D. Veraart (Eds.), *The Fascination of Probability, Statistics and their Applications: In Honour of Ole E. Barndorff-Nielsen*, pp. 29–52. Cham: Springer.
- Nourdin, I., G. Peccati, and M. Podolskij (2011). Quantitative Breuer-Major theorems. *Stochastic Processes and their Applications* 121(4), 793–812.
- Taylor, G. I. (1938). The spectrum of turbulence. *Proceedings of the Royal Society of London. Series A, Mathematical and Physical Sciences* 164(919), 476–490.
- Wu, C. F. J. (1986). Jackknife, bootstrap and other resampling methods in regression analysis. *Annals of Statistics* 14(4), 1261–1350.

A Simulation design

In our Monte Carlo study presented above we have simulated $n + 1 \in \mathbb{N}$ equidistant observations $X_0, X_{1/n}, X_{2/n}, \dots, X_1$ of the *BSS* process

$$X_t = \int_{-\infty}^t g(t-s)\sigma_s dW_s \tag{25}$$

on the time interval $[0, 1]$. Recall that we take $g(x) = x^\alpha e^{-\lambda x}$ where $\lambda > 0$ and $\alpha \in (-\frac{1}{2}, \frac{1}{2})$. Simulation of X is not straightforward as the process is typically neither Gaussian nor Markovian, which rules out both exact and recursive simulation schemes. However, as shown in [Bennedsen et al. \(2017\)](#), the process X can be simulated efficiently and accurately using the so-called *hybrid scheme*, which is based on approximating X_t by a Riemann sum plus Wiener integrals of a power function that mimicks the steep behavior of g at zero. In particular, the hybrid scheme improves significantly simulation accuracy compared to any approximation using merely Riemann sums.

To simulate the observations $X_0, X_{1/n}, X_{2/n}, \dots, X_1$, the hybrid scheme approximates $X_{i/n}$, $i = 0, 1, \dots, n$, by

$$X_{i/n}^n := \check{X}_{i/n}^n + \hat{X}_{i/n}^n,$$

where

$$\check{X}_t^n := \sum_{k=1}^{\kappa} L_g\left(\frac{k}{n}\right) \sigma_{t-k/n} \int_{t-\frac{k}{n}}^{t-\frac{k}{n}+\frac{1}{n}} (t-s)^\alpha dW_s, \quad (26)$$

$$\hat{X}_t^n := \sum_{k=\kappa+1}^{N_n} g\left(\frac{b_k^*}{n}\right) \sigma_{t-k/n} (W_{t-k/n+1/n} - W_{t-k/n}). \quad (27)$$

The number $N_n := \lfloor n^{1+\delta} \rfloor$, for some $\delta > 0$, determines the truncation "towards minus infinity", while $\kappa \geq 0$ denotes the number of terms that are simulated directly via Wiener integrals, cf. (26). As shown in [Bennedsen et al. \(2017\)](#), $\kappa = 1$ suffices when $\alpha < 0$, but we need $\kappa = 3$ when α is close to $\frac{1}{2}$. In the simulations, we therefore choose $\kappa = 1$ when $\alpha < 0$ and $\kappa = 3$ when $\alpha > 0$. We also let $\delta = 0.5$. The numbers

$$b_k^* = \left(\frac{k^{\alpha+1} - (k-1)^{\alpha+1}}{\alpha+1} \right)^{1/\alpha},$$

$k = 1, \dots, N_n$, are the optimal points⁵ to evaluate g at; see Proposition 2.2 of [Bennedsen et al. \(2017\)](#). We refer to [Bennedsen et al. \(2017\)](#) for implementation of the algorithm used to simulate (26) and (27) exactly while simulateneously simulating $\sigma_{i/n-k/n}$, $i, k = 0, 1, \dots$, which may be correlated with W .

For the stochastic volatility process $\sigma = (\sigma_t)_{t \in \mathbb{R}}$, we consider three different specifications: (i) constant volatility, labeled NoSV; (ii) one-factor stochastic volatility, labeled SV1F; and (iii) two-factor stochastic volatility, labeled SV2F. For the NoSV model we take for $t \in \mathbb{R}$,

$$\sigma_t = 1,$$

⁵In the sense of asymptotic mean-square error.

while we in the SV1F model take, following [Barndorff-Nielsen et al. \(2008\)](#),

$$\begin{aligned}\sigma_t &= \exp(\beta_0 + \beta_1 \tau_t), \\ d\tau_t &= \xi \tau_t dt + dB_t, \\ d[W, B]_t &= \rho dt,\end{aligned}$$

where B is a standard Brownian motion and $\beta_1 = 0.125$, $\xi = -0.025$, $\beta_0 = \frac{\beta_1^2}{2\xi} = -0.3125$ and $\rho = -0.3$. Lastly, for the SV2F model we take, following [Huang and Tauchen \(2005\)](#) and [Barndorff-Nielsen et al. \(2008\)](#),

$$\begin{aligned}\sigma_t &= s\text{-exp}(\beta_0 + \beta_1 \tau_{1t} + \beta_2 \tau_{2t}), \\ d\tau_{1t} &= \xi_1 \tau_{1t} dt + dB_t^1, \\ d\tau_{2t} &= \xi_2 \tau_{2t} dt + (1 + \phi \tau_{2t}) dB_t^2, \\ d[W, B^1]_t &= \rho_1 dt, \\ d[W, B^2]_t &= \rho_2 dt,\end{aligned}$$

where B^1, B^2 are standard Brownian motions and the function $s\text{-exp}$ is given by

$$s\text{-exp}(x) = \begin{cases} \exp(x), & x \leq \log(1.5), \\ \frac{3}{2} \sqrt{1 - \log(1.5) + x^2 / \log(1.5)}, & x > \log(1.5) \end{cases}$$

and the parameters are set to $(\beta_0, \beta_1, \beta_2)^T = (-1.20, 0.040, 1.50)^T$, $(\xi_1, \xi_2)^T = (-0.00137, -1.386)^T$, $\phi = 0.250$ and $\rho_1 = \rho_2 = -0.30$.

We note that in the NoSV case the process X is Gaussian and can thus be simulated exactly using a Cholesky decomposition of its variance-covariance matrix, which is what we do in our simulations. The stochastic processes of SV1F and SV2F can be simulated exactly using methods in [Glasserman \(2003\)](#), see also the Simulation Appendix to [Barndorff-Nielsen et al. \(2008\)](#).

B Expressions for Λ_p , $\lambda_{p,n}^{i,j}$, and $\mu(p, \nu)_t^n$

In both the ordinary CLT (10) as well as the bootstrap CLT there are various terms that are necessary to derive when implementing the methods. In particular, the ordinary CLT requires calculation of $\Lambda_p = \{\lambda_p^{i,j}\}_{1 \leq i, j \leq 2}$ while the bootstrap CLT requires calculation of $\{\lambda_{p,n}^{i,j}\}_{1 \leq i, j \leq 2}$ as well as $\mu(p, \nu)_t^n = \mathbb{E}^*(V(B^H; p, \nu)_t^n)$ for $\nu = 1, 2$, see Remark 2. Although the calculations involved are quite straightforward, they are tedious. For the convenience of the reader, we supply the expressions for these terms here. In what follows we denote by $n = \lfloor t/\Delta_n \rfloor$ the total number of observations.

Recall the specifications

$$\begin{aligned}\lambda_{p,n}^{11} &= \Delta_n^{-1} \text{var} \left(\bar{V} (B^H; p, 1)_1^n \right), \\ \lambda_{p,n}^{22} &= \Delta_n^{-1} \text{var} \left(\bar{V} (B^H; p, 2)_1^n \right), \\ \lambda_{p,n}^{12} &= \Delta_n^{-1} \text{cov} \left(\bar{V} (B^H; p, 1)_1^n, \bar{V} (B^H; p, 2)_1^n \right),\end{aligned}$$

and $\lambda_p^{i,j} = \lim_{n \rightarrow \infty} \lambda_{p,n}^{i,j}$. Analytical expressions are only known for $p = 2$, which is arguably the most relevant in empirical applications as it corresponds to using squared increments when calculating power variations. We therefore only consider $p = 2$ here.

Let ρ_{v_1, v_2}^H be the correlation function between the second order increments of the fractional Brownian motion with Hurst index H , calculated at lag v_1 , and the second order increment calculated at lag v_2 . In other words

$$\rho_{v_1, v_2}^H(h) := \text{Corr} (B_{i+h}^H - 2B_{i+h-v_1}^H + B_{i+h-2v_1}^H, B_i^H - 2B_{i-v_2}^H + B_{i-2v_2}^H), \quad h \in \mathbb{Z}.$$

We will need the combinations $(v_1, v_2) = (1, 1), (2, 2), (1, 2)$ and we give them for reference:

$$\begin{aligned}\rho_{1,1}^H(h) &:= \frac{1}{2(4 - 2^{2H})} (-|h - 2|^{2H} + 4|h - 1|^{2H} - 6|h|^{2H} + 4|h + 1|^{2H} - |h + 2|^{2H}), \\ \rho_{2,2}^H(h) &:= \frac{1}{2(4 \cdot 2^{2H} - 4^{2H})} (-|h - 4|^{2H} + 4|h - 2|^{2H} - 6|h|^{2H} + 4|h + 2|^{2H} - |h + 4|^{2H}), \\ \rho_{1,2}^H(h) &:= \frac{-|h - 2|^{2H} + 2|h - 1|^{2H} + |h|^{2H} - 4|h + 1|^{2H} + |h + 2|^{2H} + 2|h + 3|^{2H} - |h + 4|^{2H}}{2\sqrt{4 - 2^{2H}}\sqrt{4 \cdot 2^{2H} - 4^{2H}}}.\end{aligned}$$

Brute force calculations will yield

$$\begin{aligned}\lambda_{2,n}^{11} &= 2\Delta_n^{4H} \sum_{i=2}^n \sum_{j=2}^n \rho_{1,1}^H(i - j)^2, \\ \lambda_{2,n}^{22} &= 2\Delta_n^{4H} \sum_{i=4}^n \sum_{j=4}^n \rho_{2,2}^H(i - j)^2, \\ \lambda_{2,n}^{12} &= \lambda_{2,n}^{21} = 2\Delta_n^{4H} \sum_{i=2}^n \sum_{j=4}^n \rho_{1,2}^H(i - j)^2.\end{aligned}$$

In the feasible implementation in Remark 2 we will actually need the unnormalized variants of $\lambda_{2,n}^{i,j}$ which are

$$\begin{aligned}\text{Var} \left(V (B^H; p, 1)_1^n \right) &= \Delta_n \lambda_{2,n}^{11} \cdot (4 - 2^{2H})^2, \\ \text{Var} \left(V (B^H; p, 2)_1^n \right) &= \Delta_n \lambda_{2,n}^{22} \cdot (4 \cdot 2^{2H} - 4^{2H})^2, \\ \text{Cov} \left(V (B^H; p, 1)_1^n, V (B^H; p, 2)_1^n \right) &= \Delta_n \lambda_{2,n}^{12} \cdot (4 - 2^{2H})(4 \cdot 2^{2H} - 4^{2H}).\end{aligned}$$

To arrive at expressions for λ_p^{ij} we can either take limits in the above or use the theory in Nourdin et al. (2011) (see e.g. Barndorff-Nielsen et al., 2013) to get

$$\begin{aligned}\lambda_2^{11} &= 2 + 4 \sum_{h=1}^{\infty} \rho_{1,1}^H(h)^2, \\ \lambda_2^{22} &= 2 + 2^{-4H+2} \sum_{h=1}^{\infty} [\rho_{1,1}^H(h-2) + 4\rho_{1,1}^H(h-1) + 6\rho_{1,1}^H(h) + 4\rho_{1,1}^H(h+1) + \rho_{1,1}^H(h+2)]^2, \\ \lambda_2^{12} &= \lambda_2^{21} = 2^{3-2H} (\rho_{1,1}^H(1) + 1)^2 + 2^{2-2H} \sum_{h=0}^{\infty} [\rho_{1,1}^H(h) + 2\rho_{1,1}^H(h+1) + \rho_{1,1}^H(h+2)]^2.\end{aligned}$$

Finally, we need to calculate $\mu(2, 1)_t^n$ and $\mu(2, 2)_t^n$. Straightforward calculations yield

$$\begin{aligned}\mu(2, 1)_t^n &= (n-1)\Delta_n^{2H} (4 - 2^{2H}), \\ \mu(2, 2)_t^n &= (n-3)\Delta_n^{2H} (4 \cdot 2^{2H} - 4^{2H}).\end{aligned}$$

C Proofs

Proof of Proposition 2.1. The proofs of the statements follow the ones referenced in Corcuera et al. (2013) almost verbatim, which in turn relies on results from Barndorff-Nielsen et al. (2013). We note that in the case of $\alpha = 0$ the increments of the \mathcal{BSS} process are asymptotically uncorrelated. Indeed, we have by Assumption 2'(i) (cf. equation (2.6) in Corcuera et al., 2013)

$$r_n(j) := \text{corr}(G_{(j+1)\Delta_n} - 2G_{j\Delta_n} + G_{(j-1)\Delta_n}, G_{\Delta_n} - 2G_0 + G_{-\Delta_n}) \xrightarrow{n \rightarrow \infty} \rho_2(j), \quad j \geq 0,$$

where $\rho_2(j)$ is the correlation function of the second order increments of a Brownian motion. Therefore,

$$\rho_2(j) = 0, \quad j \geq 2.$$

This uncorrelatedness simplifies matters, for instance when we need to calculate Λ_p (see pages 85-86 in Barndorff-Nielsen et al., 2013). The proof of Proposition 2.1 has two main parts, see the similar proofs in Barndorff-Nielsen et al. (2011, 2013). First, we need to show the existence of a sequence $r(j)$, such that

$$|r_n(j)| \leq Cr(j), \quad \sum_{j=1}^{\infty} r(j)^2 < \infty, \quad (28)$$

where $C > 0$, see page 75 in Barndorff-Nielsen et al. (2013) for the case of $\alpha \neq 0$. Given that (e.g. Barndorff-Nielsen et al., 2013)

$$r_n(j) = \frac{-R\left(\frac{j+2}{n}\right) + 4R\left(\frac{j+1}{n}\right) - 6R\left(\frac{j}{n}\right) + 4R\left(\frac{j-1}{n}\right) - R\left(\frac{j-2}{n}\right)}{4R\left(\frac{1}{n}\right) - R\left(\frac{2}{n}\right)},$$

it is not difficult to show, using Assumptions 2'(i)-(iii) and the approach from the proof of Lemma 1 in [Barndorff-Nielsen et al. \(2009\)](#), that the sequence

$$r(j) = (j - 1)^{-\beta}, \quad j \geq 2,$$

will suffice as the sequence in (28), where β is the parameter from Assumption 2'(ii). We now turn to the second part of the proof. Define

$$\pi^n(A) := \frac{\int_A (g(x + 2\Delta_n) - 2g(x + \Delta_n) + g(x))^2 dx}{\int_0^\infty (g(x + 2\Delta_n) - 2g(x + \Delta_n) + g(x))^2 dx}, \quad A \in \mathcal{B}(\mathbb{R}).$$

The only remaining thing to show is to ensure that the limit theorems apply for stochastic σ , is that for all $\epsilon > 0$ we have $\pi^n((\epsilon, \infty)) \rightarrow 0$ as $n \rightarrow \infty$. Using Assumption 1' (ii) and arguments as the ones in [Barndorff-Nielsen et al. \(2013\)](#) page 74, we easily deduce this property. This concludes the proof. ■

Proof of Lemma 3.1. (i) Given (1), (13), and (14) the result follows. In particular, we have that

$$\begin{aligned} \mathbb{E}^* \left(\bar{V}^* (X, B^H; p, v)_t^n \right) &= \frac{|\hat{\sigma}(p, v)_t^n|^p}{\bar{\mu}(p, v)_t^n} \mathbb{E}^* \left(\bar{V} (B^H; p, v)_t^n \right) \\ &= |\hat{\sigma}(p, v)_t^n|^p \end{aligned}$$

(ii) Given (1), (13), and (14), we can write

$$\begin{aligned} &Var^* \left(\Delta_n^{-1/2} \bar{V}^* (X, B^H; p, 1)_t^n \right) \\ &= \Delta_n^{-1} \left(\frac{|\hat{\sigma}(p, 1)_t^n|^p}{\bar{\mu}(p, 1)_t^n} \right)^2 Var^* \left(\bar{V} (B^H; p, 1)_t^n \right). \end{aligned}$$

(iii) Follows similarly as the proof of Lemma 3.1 part (ii). (iv) Given (14), we can write

$$\begin{aligned} &Cov^* \left(\Delta_n^{-1/2} \bar{V}^* (X, B^H; p, 1)_t^n, \Delta_n^{-1/2} \bar{V}^* (X, B^H; p, 2)_t^n \right) \\ &= \Delta_n^{-1} \left(\frac{|\hat{\sigma}(p, 1)_t^n|^p}{\bar{\mu}(p, 1)_t^n} \right) \left(\frac{|\hat{\sigma}(p, 2)_t^n|^p}{\bar{\mu}(p, 2)_t^n} \right) Cov \left(\bar{V} (B^H; p, 1)_t^n, \bar{V} (B^H; p, 2)_t^n \right). \end{aligned}$$

(iv) This result follows immediately given parts (ii), (iii), and (iv) of Lemma 3.1, the assumed condition $|\hat{\sigma}(p, v)_t^n|^{2p} \xrightarrow{u.c.p.} \int_0^1 |\sigma_s|^{2p} ds$, and the definition of $\tilde{\Lambda}_{p,t}^n$. ■

Proof of Theorem 3.1. Note that we can write

$$\hat{\mathbf{S}}_n^* = \hat{A}_n^* \mathbf{S}_n^*,$$

where \mathbf{S}_n^* is given by

$$\mathbf{S}_n^* = \left(\Sigma^* (X, B^H; p)_t^n \right)^{-1/2} (\Delta_n)^{-1/2} \begin{pmatrix} \bar{V}^* (X, B^H; p, 1)_t^n - \mathbb{E}^* \left(\bar{V}^* (X, B^H; p, 1)_t^n \right) \\ \bar{V}^* (X, B^H; p, 2)_t^n - \mathbb{E}^* \left(\bar{V}^* (X, B^H; p, 2)_t^n \right) \end{pmatrix},$$

and

$$\hat{A}_n^* = \left(\hat{\Sigma}^* (X, B^H; p)_t^n \right)^{-1/2} \left(\Sigma^* (X, B^H; p)_t^n \right)^{1/2}.$$

Hence, to obtain the desired result of $\widehat{\mathbf{S}}_n^*$, we may proceed in two steps:

Step 1. Show that $\mathbf{S}_n^* \xrightarrow{d^*} N(0, I_2)$.

Step 2. Show that $\widehat{A}_n^* \xrightarrow{\mathbb{P}^*} I_2$.

For Step 1, note that we can write \mathbf{S}_n^* as follows

$$\mathbf{S}_n^* = \left(\Sigma^* (X, B^H; p)_t^n \right)^{-1/2} D \cdot \mathbf{T}_n$$

where

$$D = \begin{pmatrix} \frac{|\widehat{\sigma}(p,1)_t^n|^p}{\bar{\mu}(p,1)_t^n} & 0 \\ 0 & \frac{|\widehat{\sigma}(p,2)_t^n|^p}{\bar{\mu}(p,2)_t^n} \end{pmatrix},$$

and

$$\mathbf{T}_n = (\Delta_n)^{-1/2} \begin{pmatrix} \bar{V}(B^H; p, 1)_t^n - \mathbb{E}(\bar{V}(B^H; p, 1)_t^n) \\ \bar{V}(B^H; p, 2)_t^n - \mathbb{E}(\bar{V}(B^H; p, 2)_t^n) \end{pmatrix}.$$

Under our assumptions, we have that (Breuer and Major, 1983, Theorem 1)

$$\mathbf{T}_n \xrightarrow{d} N(0, \Lambda_p).$$

Thus, results in Step 1 will follow if we can show that

$$\left(\Sigma^* (X, B^H; p)_t^n \right)^{-1/2} D = \left(D^{-1} \left(\Sigma^* (X, B^H; p)_t^n \right)^{1/2} \right)^{-1} \xrightarrow{\mathbb{P}^*} \Lambda_p^{-1/2}.$$

To this end, note that we have

$$D^{-1} \left(\Sigma^* (X, B^H; p)_t^n \right)^{1/2} = \begin{pmatrix} \sqrt{\lambda_{p,n}^{11}} & 0 \\ \frac{\lambda_{p,n}^{12}}{\sqrt{\lambda_{p,n}^{11}}} & \sqrt{\lambda_{p,n}^{22} - \frac{(\lambda_{p,n}^{12})^2}{\lambda_{p,n}^{11}}} \end{pmatrix} \equiv \Theta_{p,n},$$

where we use

$$D^{-1} = \begin{pmatrix} \frac{\bar{\mu}(p,1)_t^n}{|\widehat{\sigma}(p,1)_t^n|^p} & 0 \\ 0 & \frac{\bar{\mu}(p,2)_t^n}{|\widehat{\sigma}(p,2)_t^n|^p} \end{pmatrix},$$

and

$$\begin{aligned} & \left(\Sigma^* (X, B^H; p)_t^n \right)^{1/2} \\ &= \begin{pmatrix} \sqrt{(\bar{\mu}(p,1)_t^n)^{-2} \lambda_{p,n}^{11} |\widehat{\sigma}(p,1)_t^n|^{2p}} & 0 \\ \frac{(\bar{\mu}(p,2)_t^n)^{-1} \lambda_{p,n}^{12} |\widehat{\sigma}(p,2)_t^n|^p}{\sqrt{\lambda_{p,n}^{11}}} & \sqrt{(\bar{\mu}(p,2)_t^n)^{-2} \lambda_{p,n}^{22} |\widehat{\sigma}(p,2)_t^n|^{2p} - \frac{(\bar{\mu}(p,2)_t^n)^{-2} (\lambda_{p,n}^{12})^2 |\widehat{\sigma}(p,2)_t^n|^{2p}}{\lambda_{p,n}^{11}}} \end{pmatrix}. \end{aligned}$$

The result follows since

$$\Theta_{p,n} \Theta_{p,n}^T = \Lambda_{p,n} = \begin{pmatrix} \lambda_{p,n}^{11} & \lambda_{p,n}^{12} \\ \lambda_{p,n}^{12} & \lambda_{p,n}^{22} \end{pmatrix} \rightarrow \Lambda_p.$$

For Step 2, it suffices to show that

$$\left(\widehat{\Sigma}^*(X, B^H; p)_t^n\right)^{-1} \left(\Sigma^*(X, B^H; p)_t^n\right) = \left(\left(\Sigma^*(X, B^H; p)_t^n\right)^{-1} \left(\widehat{\Sigma}^*(X, B^H; p)_t^n\right)\right)^{-1} \xrightarrow{\mathbb{P}^*} I_2.$$

We here utilize the fact that convergence in L_1 implies convergence in probability and that all elements of the sum in $\widehat{\Sigma}_{i,j}^*$ are non-negative (where $\widehat{\Sigma}_{i,j}^*$ is the (i, j) -th element of the matrix $\widehat{\Sigma}^* = \left(\widehat{\Sigma}_{i,j}^*\right)_{1 \leq i, j \leq 2}$). In particular, given (20) and (19), for $1 \leq i, j \leq 2$, we have

$$\mathbb{E}^* \left| \widehat{\Sigma}_{i,j}^* \right| = \mathbb{E}^* \left(\widehat{\Sigma}_{i,j}^* \right) = \Sigma_{i,j}^*.$$

Thus, we deduce that

$$\widehat{\Sigma}^*(X, B^H; p)_t^n - \Sigma^*(X, B^H; p)_t^n \xrightarrow{\mathbb{P}^*} 0.$$

This concludes the proof of Step 2 and also that of Theorem 3.1. ■

Proof of Theorem 3.2. Given Theorem 3.1, the result follows from an application of the delta method. ■